

All loop structures in Supergravity Amplitudes on $AdS_5 \times S^5$ from CFT

Agnese Bissi¹, Giulia Fardelli¹, Alessandro Georgoudis^{1,2,3}

¹*Department of Physics and Astronomy, Uppsala University Box 516, SE-751 20 Uppsala, Sweden*

²*Institut de Physique Théorique, CEA, CNRS, Université Paris-Saclay, F-91191 Gif-sur-Yvette cedex, France*

³*Laboratoire de physique de l'Ecole normale supérieure, ENS, Université PSL, CNRS, Sorbonne Université, Université Paris-Diderot, Sorbonne Paris Cité, 24 rue Lhomond, 75005 Paris, France*

Abstract

We compute a set of structures which appear in the four-point function of protected operators of dimension two in $\mathcal{N} = 4$ Super Yang Mills with $SU(N)$ gauge group, at any order in a large N expansion. They are determined only by leading order CFT data. By focusing on a specific limit, we make connection with the dual supergravity amplitude in flat space, where such structures correspond to iterated s -cuts. We make several checks and we conjecture that the same interpretation holds for supergravity amplitudes on $AdS_5 \times S^5$.

Contents

1	Introduction and summary	2
2	Four-point function	6
2.1	$\langle \mathcal{O}_2 \mathcal{O}_2 \mathcal{O}_2 \mathcal{O}_2 \rangle$ correlator	7
2.2	Leading logarithmic singularities	10
2.3	Double Discontinuity and flat space limit	12
2.4	Flat space limit of higher logarithmic terms at all loops	14
3	Four-graviton scattering amplitude	17
3.1	The two loop example as the starting point	18
3.2	Higher Loop generalisation	20
4	Mellin space	24
4.1	Generalities and flat space limit	24
4.2	Two loops and beyond	25
A	Harmonic Polylogarithms	28
B	The two loop example	28
B.1	Results for $\mathcal{H}^{(3)} _{\log^3(z\bar{z})}$	29
B.2	Two loop SUGRA Amplitude	30
B.3	Match Amplitude and CFT at 2 loops	33
B.4	Two-loop Mellin amplitude	35
C	Polynomial Structure	38

1 Introduction and summary

Since the advent of the AdS/CFT correspondence a lot of progress has been achieved in the computation of observables, in particular correlation functions of local and non local operators or equivalently scattering amplitudes of the dual string states. Despite the huge effort, there is not yet a working strategy to compute the above-mentioned observables in four dimensional $\mathcal{N}=4$ Super Yang Mills (SYM) with gauge group $SU(N)$, for generic values of the coupling constant g_{YM} and of the number of colours N . In this paper we make use of the holographic dictionary and of the symmetry group of $\mathcal{N}=4$ SYM to find structures which appear in the four-point correlation function of protected operators of dimension two, for large 't Hooft coupling $\lambda = g_{YM}^2 N$ and at all loops in the large N expansion. In this particular

regime, often called supergravity limit, we are probing the four-point graviton amplitude in the two derivative supergravity effective action and at any genus. This limit makes clear the fact that traditional techniques such as diagrammatic Witten diagram computations are generically very hard or even impossible to be carried out. In the last years there has been a considerable progress in computing such observables combining the methods of the analytic bootstrap, localization, and integrability [1–19]. In particular it has been possible to compute the four-point function of half-BPS operators of protected dimension two \mathcal{O}_2 , in a large N expansion up to order $\frac{1}{N^4}$ and as an expansion in inverse powers of λ . In the supergravity regime, the intermediate states in the operator product expansion (OPE) of $\mathcal{O}_2 \times \mathcal{O}_2$ are double trace operators of the schematic form $[\mathcal{O}_2 \mathcal{O}_2]_{n,\ell} \sim \mathcal{O}_2 \square^n \partial^\ell \mathcal{O}_2$ with dimension $\Delta_{n,\ell} = 4 + 2n + \ell + \frac{\gamma_{n,\ell}^{(1)}}{N^2} + \frac{\gamma_{n,\ell}^{(2)}}{N^4} + \dots$. To compute the anomalous dimension $\gamma_{n,\ell}^{(2)}$ it has been crucial to notice that at leading order there is a degeneracy among the different double trace operators of the form $[\mathcal{O}_p \mathcal{O}_p]_{n,\ell}$ which have bare dimension $2p + 2n + \ell$. Up to order $\frac{1}{N^2}$ the mixing has been solved, which means that both the square of the three-point functions $a_{n,\ell,I}^{(0)} \sim \langle \mathcal{O}_2 \mathcal{O}_2 \mathcal{O}_{n,\ell,I} \rangle$ and the anomalous dimensions $\gamma_{n,\ell,I}^{(1)}$ have been computed, where $\mathcal{O}_{n,\ell,I}$ denotes the eigenstate of the dilatation generator which is a specific linear combination of the double trace operators $[\mathcal{O}_p \mathcal{O}_p]_{n,\ell}$ [20–22]. In addition, up to order $\frac{1}{N^4}$ the double discontinuity (dDisc) of the four-point function is completely determined by $a_{n,\ell,I}^{(0)}$ and $\gamma_{n,\ell,I}^{(1)}$, thus making possible to compute the four-point function at this order, also including corrections in inverse power of λ^1 . One interesting comment to make is that in all studied cases, there has been a matching between a specific limit in the correlation function, which is the one probing the bulk point singularity, and the flat space limit of the amplitude [11].

Going higher in the $\frac{1}{N}$ expansion has several difficulties, both technical and conceptual. The first one is that also at leading order in the 't Hooft coupling λ , there are additional operators in the OPE of $\mathcal{O}_2 \times \mathcal{O}_2$, in particular there are triple trace operators of the schematic form $[\mathcal{O}_{p_1} \mathcal{O}_{p_2} \mathcal{O}_{p_3}]$ which can potentially mix among themselves and with the double trace ones. Another obstacle resides in the fact that the dDisc gets contributions from other terms in the conformal blocks expansion which cannot be expressed in terms only of tree level and one loop CFT data. Despite these obstacles, at any given order $\frac{1}{N^{2\kappa}}$ the four-point function $\mathcal{G}^{(\kappa)}(z, \bar{z})$ contains a piece which can be fully reconstructed once we know the leading order data

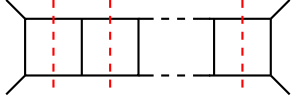
$$\log^\kappa(z\bar{z}) \sum_{I,n,\ell} \frac{a_{n,\ell,I}^{(0)} \left(\gamma_{n,\ell,I}^{(1)} \right)^\kappa}{2^\kappa \kappa!} (z\bar{z})^{n+2} g_{8+2n,\ell}(z, \bar{z}) \subset \mathcal{G}^{(\kappa)}(z, \bar{z}), \quad (1.1)$$

where the cross ratios enter as $U = z\bar{z}$ and $V = (1-z)(1-\bar{z})$, $g_{n,\ell}(z, \bar{z})$ are the four dimensional conformal blocks and $\mathcal{G}^{(\kappa)}(z, \bar{z})$ is the four-point function at order $\frac{1}{N^{2\kappa}}$ ². The main idea of our work is to understand to which part of the dual amplitude this piece corresponds to at any given κ order. To get to this relationship we study the bulk point limit and put it in relation with the flat space limit of the corresponding amplitude, by comparing the discontinuities of the two observables. In a previous work [10] we have unravelled the case of $\kappa = 3$ and we have seen that the double cut of the amplitude exactly reproduces the flat

¹At order $\frac{1}{N^4}$ there is a contact term like ambiguity, which only influences the CFT data corresponding to the intermediate scalar operators in the OPE.


²The precise definitions will be given later in the text.

space limit of the CFT and only conjectured that the same behaviour would persist at any loop order. In this paper we have substantiated this observation and we have constructed the iterated s -cut to all loops. We have found that the bulk point limit of the double discontinuity of the leading logarithmic term in $\mathcal{G}^{(\kappa)}$, once logarithms are factored out, is reproduced by the iterated s -channel cut of the corresponding κ rungs ladder diagram. Pictorially this reads

$$\sum_{n,\ell} \sum_{I=1}^{n+1} (z\bar{z})^{n+2} a_{n,\ell,I}^{(0)} (\gamma_{n,\ell,I}^{(1)})^\kappa g_{2n+8,\ell}(z, \bar{z}) \xleftrightarrow{\text{flat space}} \text{Diagram} \quad (1.2)$$


This allowed us to notice some interesting features on how the unitarity structure translates in the flat-space limit. First of all when studying the discontinuity of the amplitude, it is evident the appearance of multi-particle states in the cuts one has to construct, thus suggesting the need to include higher and higher trace operators in the OPE in the large N expansion of the correlator. At two loops we have noticed that the structure of the double particle contribution in the amplitude is fixed by its iterated s -cut construction contrary to the correlator where the knowledge of the $\log^2 U$ part can not be fully reconstructed. The most important remark that we would like to make at this point is the fact that we expect such s -channel cutting holds also in the full-fledged amplitudes in the $AdS_5 \times S^5$ background, on the line also of [23, 24].

An interesting interpretation of the iterated cut depicted before, which formally can be written as the corresponding Feynman integral with insertions of delta functions for each cut propagator as in Eq. (3.13), can be given when considering the theory of Landau singularities [25]. In this context in fact, this quantity measures the discontinuity of the *lower-order* Landau singularity associated to κ contractions. A *lower-order* Landau singularity is defined as the *leading singularity* of a contracted graph, a Feynman diagram where all the internal legs, that are not on-shell, are pinched together to a point. In our specific case,

$$\text{lower-order singularity associated to } \kappa \text{ contractions} \quad \Leftrightarrow \quad \text{leading singularity of } \text{Diagram}$$


Finally from our analysis in Mellin space, it emerges even more clearly the interplay between unitarity cuts of flat space amplitudes and CFT correlator with a certain logarithmic behaviour in the small U and V expansion. In particular we conjecture that the Mellin amplitude corresponding to the leading logarithmic terms at a given κ order and in the large AdS radius limit can be derived from a *maximal cut* of the corresponding ladder diagram.

In summary, in this paper we study a specific contribution of the four point correlator, which is proportional to $\log^\kappa U$, for $\kappa = 3$ we computed the full function, and for higher κ we give an explicit method to compute it. In the specific limit that we compare to the flat space limit of the amplitude, we computed this function to several values of κ , which label the loop order. Given the evidences of the explicit examples, we conjecture that at any loop order the leading logs of the four-point function, completely fixed by known tree level data, reproduce in the flat space limit iterated s -channel cuts of the dual graviton amplitude. Since only planar ladders admit exactly $(\kappa - 1)$ two-particle cuts at $(G_N)^\kappa$, we restrict our

discussion just to these diagrams. Moreover a similar analysis, performed in Mellin space, enables us to establish a connection between the residues of $(s - 2m)^{-(\kappa-1)}(t - 2n)^{-1}$ terms and maximal cuts.

Due to the appearance of higher trace operators and the unsolved mixing problem, we do not go beyond $\log^\kappa U$ contributions. Nonetheless in the specific $\kappa = 3$ example we make clear how triple trace operators enter the discussion and how to disentangle their contribution at the level of the amplitude.

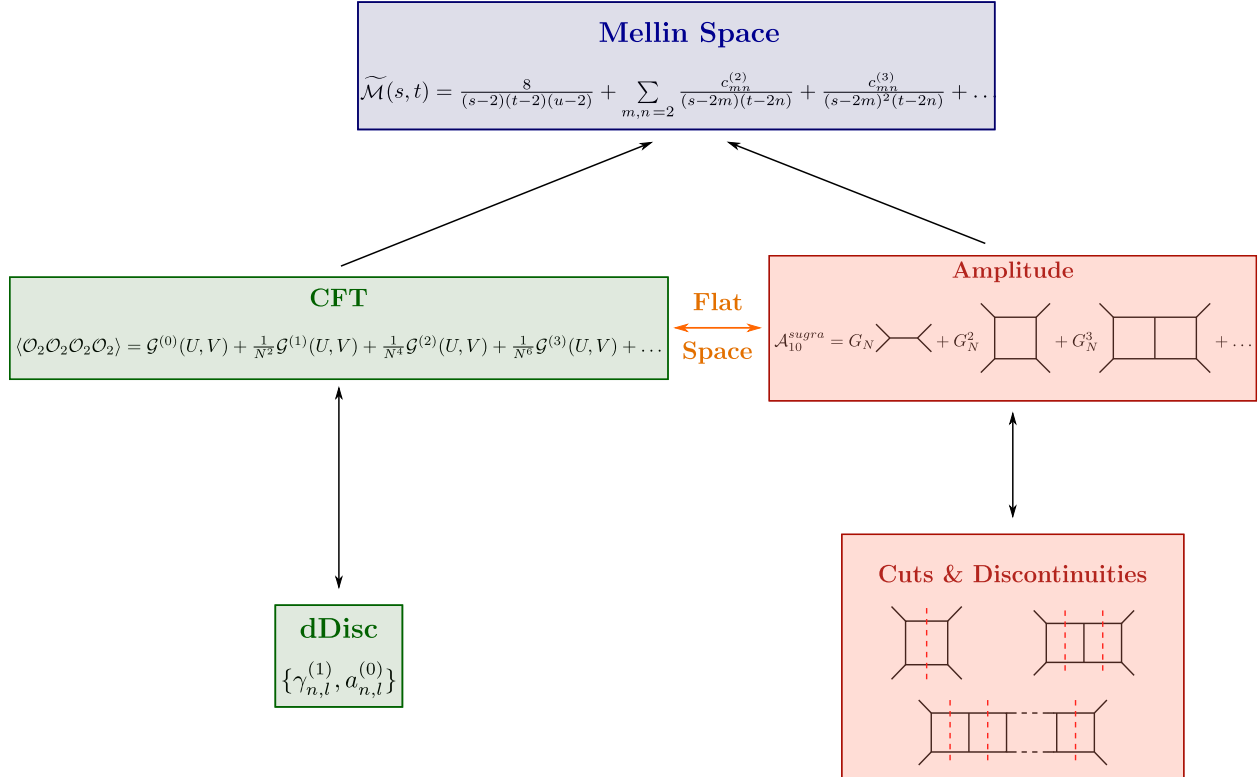


Figure 1: Visual idea of the working strategy we will be following in the paper. ³

Open questions

- **Include stringy corrections:** While we worked in a regime in which the 't Hooft coupling constant is strictly infinite, it would be interesting to add the full expansion in inverse powers of λ . This would allow including quartic vertices in the amplitudes, along the lines of [13]. We believe that the same interpretation in terms of s -cuts holds in this case as well. Going beyond the supergravity limit would also require the introduction of single trace operators in the OPE, in addition to the double trace and higher trace operators which are already taken into account. Enlarging the set of operators will make possible to go away from the strong coupling regime and probe finite coupling.
- **Resum iterated $(\kappa - 1)$ -cut:** Given the simplicity and the iterative form of multiple s -cuts for ladder diagrams, it would be interesting to resum this contribution to all orders and explore possible physical interpretation. This seems reminiscent of leading Regge behaviour of four-point amplitudes. A similar behaviour has been extensively studied in QCD and solved using a Wilson line approach [26].
- **Complement our results with string theory computations:** Low energy expansion of string theory amplitudes has a revival in the last years. In particular old fashioned methods have been complemented with insights from modular graph forms and the closed/open string amplitudes relations, along the lines of [27–33]. In the spirit of computing string amplitudes, at any value of the central charge and of the 't Hooft coupling, the synergy of these methods can be helpful and can provide insights that can be useful in both methods.

The paper is organised as follows. In Section 2 we study the $\langle \mathcal{O}_2 \mathcal{O}_2 \mathcal{O}_2 \mathcal{O}_2 \rangle$ correlation function in the large N expansion focusing on its leading logarithmic terms in the flat space limit. The corresponding quantity on the gravity side, namely the supergravity four-graviton amplitude in \mathbb{R}^{10} , is at the centre of Section 3. Here we very briefly collect the main findings for the two-loop example and, starting from them, we extend the results to all loops introducing the idea of iterated s -channel unitarity cuts. In Section 4 we address similar problems, but now rephrased in Mellin space. Some Appendices collect the lengthier computations and other technical details, in particular in Appendix B a full analysis of the two-loop correlator is given, complementing the discussion of our previous work [10].

2 Four-point function

In this paper we focus on the study of the four-point correlation function of dimension two protected operators in $\mathcal{N} = 4$ SYM in four dimensions with gauge group $SU(N)$. These are the lowest dimension half-BPS operators \mathcal{O}_p : superconformal primary operators with protected dimension $\Delta = p$, scalars under the Lorentz group and transforming in the $[0, p, 0]$

³Notice that on the amplitude side we are not explicitly reporting the disconnected part, which is dual to the $\mathcal{G}^{(0)}$ term in the CFT correlator.

representation of the R-symmetry group $SU(4)_R \simeq SO(6)_R$. In terms of the six scalar fields Φ^i ($i = 1, \dots, 6$) of $\mathcal{N} = 4$ theory, they can be written as *single trace* operators of the form

$$\mathcal{O}_p(x, y) = y_{i_1} \dots y_{i_p} \text{Tr} \Phi(x)^{i_1} \dots \Phi(x)^{i_p} \quad p = 2, 3, \dots \quad (2.1)$$

Here we have introduced the $SO(6)$ null vectors y_i , $y \cdot y = 0$, such that the \mathcal{O}_p 's manifestly transform as symmetric traceless tensors. For later use, multi-trace operators will be given by normal product of single-trace ones taken such that they transform in a symmetric and traceless way.

Through the AdS/CFT dictionary half-BPS operators, or to be more precise a combination of (2.1) and multi-trace operators $\mathcal{O}(1/N)$ suppressed [7, 12, 14], are mapped to *single particle* states in AdS.

2.1 $\langle \mathcal{O}_2 \mathcal{O}_2 \mathcal{O}_2 \mathcal{O}_2 \rangle$ correlator

The \mathcal{O}_2 operator at the centre of our investigation represents the superconformal primary of the stress tensor multiplet: it is a scalar with $\Delta = 2$ and it transforms under the $\mathbf{20}'$ representation of $SU(4)_R$. On the gravity side it maps directly to a single particle state, the scalar belonging to the graviton multiplet in type IIB closed strings in $\text{AdS}_5 \times S^5$ background, while the \mathcal{O}_p 's with $p > 2$ correspond to Kaluza Klein modes.

Conformal invariance and supersymmetry highly constrain the form of its four-point function [34, 35]:

$$\langle \mathcal{O}_2(x_1, y_1) \mathcal{O}_2(x_2, y_2) \mathcal{O}_2(x_3, y_3) \mathcal{O}_2(x_4, y_4) \rangle = \frac{(y_1 \cdot y_2)^2 (y_3 \cdot y_4)^2}{x_{12}^4 x_{34}^4} \sum_{\mathcal{R}} Y^{\mathcal{R}}(\sigma, \tau) \mathcal{G}^{\mathcal{R}}(U, V), \quad (2.2)$$

with $x_{ij} = x_i - x_j$ and where we have defined respectively the position and polarization space cross-ratios as

$$U = \frac{x_{12}^2 x_{34}^2}{x_{13}^2 x_{24}^2} = z \bar{z}, \quad V = \frac{x_{14}^2 x_{23}^2}{x_{13}^2 x_{24}^2} = (1 - z)(1 - \bar{z}), \quad (2.3)$$

$$\sigma = \frac{(y_1 \cdot y_3)(y_2 \cdot y_4)}{(y_1 \cdot y_2)(y_3 \cdot y_4)}, \quad \tau = \frac{(y_1 \cdot y_4)(y_2 \cdot y_3)}{(y_1 \cdot y_2)(y_3 \cdot y_4)}. \quad (2.4)$$

$Y^{\mathcal{R}}(\sigma, \tau)$ are $SO(6)_R$ harmonics and the sum runs over all possible representations $\mathcal{R} \in [0, 2, 0] \otimes [0, 2, 0] = [0, 0, 0] \oplus [0, 2, 0] \oplus [0, 4, 0] \oplus [1, 0, 1] \oplus [1, 2, 1] \oplus [2, 0, 2]$. However thanks to superconformal Ward identities [36], one can actually reduce the study of the $\mathcal{G}^{\mathcal{R}}$ to only one function, namely $\mathcal{G}(U, V) \equiv \frac{\mathcal{G}^{\mathbf{105}}}{U^2}$ with $\mathbf{105} = [0, 4, 0]$. This function should fulfil the crossing symmetry condition

$$V^2 \mathcal{G}(U, V) - U^2 \mathcal{G}(V, U) + (U^2 - V^2) + \frac{U - V}{c} = 0, \quad (2.5)$$

where c represents the central charge. From the function $\mathcal{G}(U, V)$ one can further disentangle the contributions from protected and non protected operators in the Operator Product Expansion (OPE), such that

$$\mathcal{G}(U, V) = \mathcal{G}^{short}(U, V) + \mathcal{H}(U, V), \quad (2.6)$$

where $\mathcal{G}^{short}(U, V)$ is fully known and c^{-1} exact [36], and receives only contributions from the protected sector consisting of short and semi-short multiplets. The interacting and coupling dependent part $\mathcal{H}(U, V)$ admits an expansion in superconformal blocks of the form

$$\mathcal{H}(z, \bar{z}) = \sum_{\tau, \ell} a_{\tau, \ell} (z\bar{z})^{\tau/2} g_{\tau+4, \ell}(z, \bar{z}). \quad (2.7)$$

The sum runs over non protected long primaries with twist, dimension minus the spin, τ , even spin ℓ and which are singlet under $SU(4)_R$. $a_{\tau, \ell}$ indicates the square of the OPE coefficient and the superconformal blocks are defined as

$$g_{\tau, \ell} = \frac{z^{\ell+1} k_{\tau+2\ell}(z) k_{\tau-2}(\bar{z}) - \bar{z}^{\ell+1} k_{\tau+2\ell}(\bar{z}) k_{\tau-2}(z)}{z - \bar{z}}, \quad (2.8)$$

$$k_{\beta}(x) = {}_2F_1\left(\frac{\beta}{2}, \frac{\beta}{2}, \beta; x\right). \quad (2.9)$$

We study the four-point function in the supergravity regime, i.e. when the 't Hooft coupling $\lambda = g_{YM}^2 N$ is taken to infinity, and as an expansion at large N or equivalently at large $c = \frac{N^2-1}{4}$:

$$\mathcal{H}(z, \bar{z}) = \mathcal{H}^{(0)}(z, \bar{z}) + \frac{1}{c} \mathcal{H}^{(1)}(z, \bar{z}) + \frac{1}{c^2} \mathcal{H}^{(2)}(z, \bar{z}) + \frac{1}{c^3} \mathcal{H}^{(3)}(z, \bar{z}) + \dots, \quad (2.10)$$

where $\mathcal{H}^{(1)}(z, \bar{z}) = -(z\bar{z})^2 \bar{D}_{2,4,2,2}(z, \bar{z})$ [37, 38]. The crossing condition (2.5) now takes two different forms, for $\kappa = 0, 1$:

$$\begin{aligned} & (1-z)^2(1-\bar{z})^2 \mathcal{G}^{short}(z, \bar{z}) - z^2 \bar{z}^2 \mathcal{G}^{short}(1-z, 1-\bar{z}) + (z^2 \bar{z}^2 - (1-z)^2(1-\bar{z})^2) = \\ & - \frac{z\bar{z} - (1-z)(1-\bar{z})}{c} + \sum_{\kappa=0}^1 \left(-(1-z)^2(1-\bar{z})^2 \frac{\mathcal{H}^{(\kappa)}(z, \bar{z})}{c^{\kappa}} + z^2 \bar{z}^2 \frac{\mathcal{H}^{(\kappa)}(1-z, 1-\bar{z})}{c^{\kappa}} \right), \end{aligned} \quad (2.11)$$

while for $\kappa \geq 2$,

$$(1-z)^2(1-\bar{z})^2 \mathcal{H}^{(\kappa)}(z, \bar{z}) = z^2 \bar{z}^2 \mathcal{H}^{(\kappa)}(1-z, 1-\bar{z}). \quad (2.12)$$

In the supergravity limit and up to order c^{-1} the only long operators exchanged in the OPE are double trace operators, whose OPE data admit an expansion similar to Eq. (2.10),

$$\tau_{n, \ell} = 4 + 2n + \frac{1}{c} \gamma_{n, \ell}^{(1)} + \frac{1}{c^2} \gamma_{n, \ell}^{(2)} + \frac{1}{c^3} \gamma_{n, \ell}^{(3)} + \dots, \quad (2.13)$$

$$a_{n, \ell} = a_{n, \ell}^{(0)} + \frac{1}{c} a_{n, \ell}^{(1)} + \frac{1}{c^2} a_{n, \ell}^{(2)} + \frac{1}{c^3} a_{n, \ell}^{(3)} + \dots \quad (2.14)$$

where with $\gamma_{n, \ell}^{(\kappa)}$ we will refer to the anomalous dimension at order $c^{-\kappa}$ and

$$\gamma_{n, \ell}^{(1)} = - \frac{(n+1)(n+2)(n+3)(n+4)}{(\ell+1)(2n+\ell+6)}, \quad (2.15)$$

$$a_{n, \ell}^{(0)} = \frac{\pi(\ell+1)(\ell+2n+6)\Gamma(n+3)\Gamma(\ell+n+4)}{2^{(2\ell+4n+9)}\Gamma(n+\frac{5}{2})\Gamma(\ell+n+\frac{7}{2})}. \quad (2.16)$$

Generically double trace operators are constructed from combinations of the half-BPS operators in Eq. (2.1), they are schematically indicated as $[\mathcal{O}_p \mathcal{O}_p]_{n,\ell} = (\mathcal{O}_p \square^n \partial_{\mu_1} \dots \partial_{\mu_\ell} \mathcal{O}_p - \text{traces})$ and at leading order they take their classical dimension $\Delta = 2p + 2n + \ell$. From their definition, it is clear that starting from different \mathcal{O}_p and with a different number of derivatives, one can construct more than one operator with the same twist and this will lead to a degeneracy. More specifically, all operators of the form $[\mathcal{O}_2 \mathcal{O}_2]_{n,\ell}, [\mathcal{O}_3 \mathcal{O}_3]_{n-1,\ell}, \dots, [\mathcal{O}_{n+2} \mathcal{O}_{n+2}]_{0,\ell}$ will contribute to Eq. (2.13) and having the same twist and spin and transforming under the same $SU(4)_R$ representation, they give rise to a mixing problem. Let us denote the collection of these $(n+1)$ degenerate states as $\mathcal{O}_{n,\ell,I}$ with $I = 1, \dots, n+1$. Quite remarkably, this mixing has been partially solved up to order c^{-1} [21, 22] and as a result $a_{n,\ell}^{(0)}$ and $\gamma_{n,\ell}^{(1)}$ are known for each I , concretely

$$\gamma_{n,\ell,I}^{(1)} = \frac{-4(n+1)_4(\ell+5+2I)_{n+2-2I}}{(\ell-1+2I)_{n+2-2I}(\ell+n+1)(\ell+n+6)}, \quad (2.17)$$

where $(x)_n = \frac{(x+n-1)!}{(x-1)!}$ is the Pochhammer symbol. For the three-point function we have

$$\langle \mathcal{O}_2 \mathcal{O}_2 \mathcal{O}_{n,\ell,I} \rangle^2 = a_{n,\ell,I} = a_{n,\ell}^{(0)} R_{n,\ell,I} c_{n,I}, \quad (2.18)$$

where

$$R_{n,\ell,I} = \frac{2^{-n-1}(4I+2\ell+3)(\ell+n+6)_{I-1}((I+\ell+1)_{-I+n+1})^{\text{sgn}(-I+n+1)}}{(I+\ell+\frac{5}{2})_{n+1}},$$

$$c_{n,I} = \frac{2^{-n-1}\Gamma(2I+3)\Gamma(n+1)\Gamma(-2I+2n+7)}{3\Gamma(I)\Gamma(I+2)\Gamma(n+5)\Gamma(-I+n+2)\Gamma(-I+n+4)}. \quad (2.19)$$

In this context the expressions in Eq. (2.15) and (2.16) should be interpreted as averaged values over the index I .

Plugging in Eq. (2.7) the expansions (2.13), (2.14) one can obtain the expressions for $\mathcal{H}^{(\kappa)}(z, \bar{z})$ as infinite sums over the double trace spectrum, we report the explicit form for the

first few orders:

$$\mathcal{H}^{(0)}(z, \bar{z}) = (z\bar{z})^{n+2} a_{n,\ell}^{(0)} g_{2n+8,\ell}(z, \bar{z}) \quad (2.20)$$

$$\mathcal{H}^{(1)}(z, \bar{z}) = (z\bar{z})^{n+2} \left(a_{n,\ell}^{(0)} \gamma_{n,\ell}^{(1)} \partial_n + a_{n,\ell}^{(1)} \right) g_{2n+8,\ell} + \frac{1}{2} (z\bar{z})^{n+2} \log(z\bar{z}) a_{n,\ell}^{(0)} \gamma_{n,\ell}^{(1)} g_{2n+8,\ell} \quad (2.21)$$

$$\begin{aligned} \mathcal{H}^{(2)}(z, \bar{z}) &= \frac{1}{2} (z\bar{z})^{n+2} \left(a_{n,\ell}^{(0)} \left(\left(\gamma_{n,\ell}^{(1)} \right)^2 \partial_n^2 + 2\gamma_{n,\ell}^{(2)} \partial_n \right) + 2a_{n,\ell}^{(1)} \gamma_{n,\ell}^{(1)} \partial_n + 2a_{n,\ell}^{(2)} \right) g_{2n+8,\ell} \quad (2.22) \\ &+ \frac{1}{2} (z\bar{z})^{n+2} \log(z\bar{z}) \left(\left(a_{n,\ell}^{(0)} \gamma_{n,\ell}^{(2)} + a_{n,\ell}^{(1)} \gamma_{n,\ell}^{(1)} \right) + a_{n,\ell}^{(0)} \left(\gamma_{n,\ell}^{(1)} \right)^2 \partial_n \right) g_{2n+8,\ell} \\ &+ \frac{1}{8} (z\bar{z})^{n+2} \log^2(z\bar{z}) a_{n,\ell}^{(0)} \left(\gamma_{n,\ell}^{(1)} \right)^2 g_{2n+8,\ell} \end{aligned}$$

$$\begin{aligned} \mathcal{H}^{(3)}(z, \bar{z}) &= \frac{1}{6} (z\bar{z})^{n+2} \left(6a_{n,\ell}^{(0)} \gamma_{n,\ell}^{(1)} \gamma_{n,\ell}^{(2)} \partial_n^2 + a_{n,\ell}^{(0)} \left(\gamma_{n,\ell}^{(1)} \right)^3 \partial_n^3 + 6a_{n,\ell}^{(0)} \gamma_{n,\ell}^{(3)} + \partial_n + \right. \quad (2.23) \\ &\quad \left. 3a_{n,\ell}^{(1)} \left(\gamma_{n,\ell}^{(1)} \right)^2 \partial_n^2 + 6a_{n,\ell}^{(1)} \gamma_{n,\ell}^{(2)} \partial_n + 6a_{n,\ell}^{(2)} \gamma_{n,\ell}^{(1)} \partial_n + 6a_{n,\ell}^{(3)} \right) g_{2n+8,\ell} \\ &+ \frac{1}{4} (z\bar{z})^{n+2} \log(z\bar{z}) \left(2 \left(a_{n,\ell}^{(0)} \gamma_{n,\ell}^{(3)} + a_{n,\ell}^{(1)} \gamma_{n,\ell}^{(2)} + a_{n,\ell}^{(2)} \gamma_{n,\ell}^{(1)} \right) + \right. \\ &\quad \left. \gamma_{n,\ell}^{(1)} \left(a_{n,\ell}^{(0)} \left(\gamma_{n,\ell}^{(1)} \right)^2 \left(\partial_n^2 + 4\gamma_{n,\ell}^{(2)} \partial_n \right) + 2a_{n,\ell}^{(1)} \gamma_{n,\ell}^{(1)} \partial_n \right) \right) g_{2n+8,\ell} \\ &+ \frac{1}{8} (z\bar{z})^{n+2} \log^2(z\bar{z}) \gamma_{n,\ell}^{(1)} \left(\left(2a_{n,\ell}^{(0)} \gamma_{n,\ell}^{(2)} + a_{n,\ell}^{(1)} \gamma_{n,\ell}^{(1)} \right) + a_{n,\ell}^{(0)} \left(\gamma_{n,\ell}^{(1)} \right)^2 \partial_n \right) g_{2n+8,\ell} \\ &+ \frac{1}{48} (z\bar{z})^{n+2} \log^3(z\bar{z}) a_{n,\ell}^{(0)} \left(\gamma_{n,\ell}^{(1)} \right)^3 g_{2n+8,\ell} \end{aligned}$$

The knowledge of the leading corrections to the dimension and OPE coefficient of the degenerate states has been enough to give the full four-point function at order c^{-2} [11, 20, 21], generically this does not hold at any given order in the perturbative expansion. However, a closer look to the expressions above reveals that only tree-level data are needed to compute what we called the *leading logarithmic singularities* at each $\mathcal{H}^{(\kappa)}$. Concretely, they take the general form

$$\mathcal{H}^{(\kappa)}(z, \bar{z}) \Big|_{\log^\kappa(z\bar{z})} = \frac{1}{2^\kappa \kappa!} \sum_{n,\ell} \sum_{I=1}^{n+1} (z\bar{z})^{n+2} a_{n,\ell,I}^{(0)} \left(\gamma_{n,\ell,I}^{(1)} \right)^\kappa g_{2n+8,\ell}(z, \bar{z}), \quad (2.24)$$

where only tree-level data of double trace operators enter and where we have reintroduced the explicit dependence on the mixing index I .

2.2 Leading logarithmic singularities

In principle we have all the information to compute the leading logarithmic terms in $\langle \mathcal{O}_2 \mathcal{O}_2 \mathcal{O}_2 \mathcal{O}_2 \rangle$. The difficulty is performing the sums over n , ℓ and I . To do so we will

use the method introduced in [39]. Before reviewing it, let us first comment on the general analytic structure of the correlator. Holographic CFTs with a bulk gravity dual are expected to develop a singularity, the bulk point singularity, which is probed by sending $z \rightarrow \bar{z}$ [13, 40–43], and whose behaviour is determined from the large n limit of $\gamma_{n,\ell}$. For the terms that we are going to study, one finds

$$\mathcal{H}^{(\kappa)} \Big|_{\log^\kappa z\bar{z}} = \frac{(z\bar{z})^2}{(z-\bar{z})^{a+4}} f^{(\kappa)}(z, \bar{z}) \quad (2.25)$$

where $f^{(\kappa)}$ contains functions of maximal degree of transcendentality κ with polynomial coefficients and the power a depends on the order of expansion as

$$a = 3 \underbrace{\kappa}_{\# \text{ of AdS loops}} + 5 \underbrace{(\kappa - 1)}_{\# \text{ of S loops}} . \quad (2.26)$$

Since from Eq. (2.15) $\gamma_{n,\ell}^{(1)} \sim n^3$ for $n \gg 1$, one would have naively expected only the 3κ term, where κ parametrizing the order in the c expansion can be equally viewed as counting the number of loops in AdS. However, the degeneracy among the double trace operators and the consequent presence of mixing enhance this singular behaviour determining the additional factor in Eq. (2.26), which accounts for the degrees of freedom of the internal S^5 manifold.

Let us now turn to a brief description of the results in [39] and let us start by introducing an eight-order differential operator $\Delta^{(8)}$ ⁴:

$$\Delta^{(8)} \equiv \frac{z\bar{z}}{(z-\bar{z})} \mathcal{D}_z (\mathcal{D}_z - 2) \mathcal{D}_{\bar{z}} (\mathcal{D}_{\bar{z}} - 2) \frac{(z-\bar{z})}{z\bar{z}} , \quad (2.27)$$

where

$$\mathcal{D}_x \equiv x^2 \partial_x (1-x) \partial_x . \quad (2.28)$$

The importance of this operator relies on the fact that when it acts on superconformal blocks, as shown in [12, 39], its eigenvalues are equal to half of the anomalous dimension of double trace operators, i.e.⁵

$$\Delta^{(8)} (u^{\tau/2} g_{\tau+4,\ell}(z, \bar{z})) = -2(n+1)_4 (\ell+n+2)_4 (u^{\tau/2} g_{\tau+4,\ell}(z, \bar{z})) . \quad (2.30)$$

This remarkable property is conjectured to descend from an accidental 10-dimensional conformal symmetry $SO(10,2)$ of the underlying supergravity amplitudes. Motivated by this symmetry, one discovers that ten dimensional blocks actually diagonalize the mixing

⁴With respect to Eq. (3.15) in [39] we are restricting directly to the case $r=0=s$ and no dependence on the $SU(4)_R$ cross-ratios. This simplification applies to the case of a correlator of four identical \mathcal{O}_2 operators.

⁵It is convenient to rewrite

$$\gamma_{n,\ell,I}^{(1)} = \frac{-4(n+1)_4 (\ell+n+2)_4}{(\ell+2I-1)_6} . \quad (2.29)$$

problem at order c^{-1} and can be used to express the leading logarithmic terms in Eq. (2.24) in a closed form, see [39] for more details,

$$\mathcal{H}^{(\kappa)}(z, \bar{z}) \Big|_{\log^\kappa(z\bar{z})} = [\Delta^{(8)}]^{\kappa-1} (\mathcal{D}_{(3)} h^{(\kappa)}(z) + z \leftrightarrow \bar{z}) , \quad (2.31)$$

where the operator $\mathcal{D}_{(3)}$ is used to build ten-dimensional blocks and it is defined as

$$\mathcal{D}_{(3)} = \left(\frac{z\bar{z}}{\bar{z}-z} \right)^7 + \left(\frac{z\bar{z}}{\bar{z}-z} \right)^6 \frac{z^2}{2} \partial_z + \left(\frac{z\bar{z}}{\bar{z}-z} \right)^5 \frac{z^3}{10} \partial_z^2 z + \left(\frac{z\bar{z}}{\bar{z}-z} \right)^4 \frac{z^4}{120} \partial_z^3 z^2 . \quad (2.32)$$

Finally,

$$h^{(\kappa)}(z) = \frac{1}{\kappa!} \left(-\frac{1}{2} \right)^\kappa \sum_{\ell=0, \text{ even}}^{\infty} \frac{960 \Gamma(\ell+1) \Gamma(\ell+4) z^{\ell+1} {}_2F_1(\ell+1, \ell+4; 2\ell+8; z)}{\Gamma(2\ell+7) [(\ell+1)_6]^{\kappa-1}} . \quad (2.33)$$

Thus in principle we have an explicit expression to compute higher logarithmic terms at a given loop order. Although we were able to develop a simple algorithm to find all the $h^{(\kappa)}$ resumming Eq. (2.33), applying $\Delta^{(8)}$ still remains a technically involving task, given the growing number of derivatives one needs to take. However, as we will discuss in the following, no derivatives are needed once one is only interested in the bulk point limit of the correlation function.

2.3 Double Discontinuity and flat space limit

The study of the flat space or equivalently the bulk point limit of correlation functions has been initiated in the works [40, 42, 43] and it is interesting for at least two reasons. First of all it can provide an insight on the analytic structure of the four-point function, secondly in this regime and for infinite 't Hooft coupling, CFT correlators can be mapped to scattering amplitudes in type IIB supergravity in the flat \mathbb{R}^{10} , which are in general more accessible and easier to compute. Our goal is to provide a general formula for the leading logarithmic term in this limit and at any order in the $c^{-\kappa}$ expansion. In doing so, we will generalize the results in [11], where it is shown that at one loop, there exists a one to one correspondence between the *discontinuity* of the non-analytic piece of the four-graviton amplitude in \mathbb{R}^{10} and the flat space limit of the *double discontinuity* (dDisc) of $\mathcal{H}^{(2)}(z, \bar{z})$.

Double Discontinuity

The dDisc of an amplitude $\mathcal{H}(z, \bar{z})$ is defined as the difference between the Euclidean correlator and its two possible analytic continuations around $\bar{z} = 1$, keeping z fixed:

$$\text{dDisc} \mathcal{H}(z, \bar{z}) \equiv \mathcal{H}(z, \bar{z}) - \frac{1}{2} (\mathcal{H}^\circlearrowleft(z, \bar{z}) + \mathcal{H}^\circlearrowright(z, \bar{z})) . \quad (2.34)$$

This quantity can be computed exploiting crossing symmetry and passing to the t -channel, where it acts trivially. Here, the only terms in the correlator $\mathcal{H}^{(k)}$ with non vanishing dDisc are $\log^n(1 - \bar{z})$, with $n \geq 2$ ($n \leq \kappa$), which are completely determined by OPE data at order $\kappa - 1$. Then, through the Lorentzian inversion formula [44], this quantity allows to reconstruct

the full correlation function. By crossing $\log(1 - \bar{z})$ corresponds to $\log(z\bar{z})$, hence at each order the leading logarithmic term in Eq. (2.24) will contribute to dDisc as

$$\text{dDisc}[\log^\kappa(1 - \bar{z})] = 2\pi^2 \kappa(\kappa - 1) \log^{\kappa-2}(1 - \bar{z}) + \text{lower powers of } \log(1 - \bar{z}). \quad (2.35)$$

Unfortunately for $\kappa \geq 3$, also lower transcendental pieces contributes to the dDisc and other contributions should be considered to reconstruct the full correlator, even in the flat space limit. For $\kappa \geq 3$ an additional obstacle to the complete reconstruction of $\mathcal{H}^{(k)}$ is the appearance of multi-trace operators, besides the double trace that we are already considering. Their emergence should become clearer later on in our discussion, when we will study the dual scattering amplitude at two loops and we will analyse the origin of its discontinuities. The $\kappa = 2$ example in [11, 13] is eventually a very special one, in this case in fact the only term entering dDisc is (2.24), thus allowing to successfully compute the whole $\mathcal{H}^{(2)}$. The main focus of this paper is to understand what can be inferred from the knowledge of this piece of information at higher order and which conclusions can we draw about its relation to the four-graviton amplitude.

Bulk point limit

Let us now pass to properly discuss the *flat space* or *bulk point limit* of correlators and its implications both on the CFT and on the gravity side. Consider sufficiently localized wave-packets in AdS, such that it can be approximated with flat space, then bulk S-matrix elements in this limit can be reproduced by correlators in the boundary CFT with a prescribed singular behaviour. In particular, to reproduce the bulk kinematics, the CFT correlation function must diverge at $z \rightarrow \bar{z}$. Notice that this type of singularity can manifest itself only in Lorentzian signature, where z and \bar{z} are real and independent variables, so to reach the bulk point limit it is needed to analytically continue the Euclidean correlator to imaginary times and then take this Lorentzian time to π . In doing so, the correlation function picks an additional phase, while the OPE expansion still holds,

$$\mathcal{H}(z, \bar{z})_{\text{Lorentzian}} = \sum_{\Delta, \ell} e^{-i\pi(\Delta - \ell)} a_{\Delta, \ell} g_{\Delta, \ell}(z, \bar{z}). \quad (2.36)$$

In large N theories, where this sum is over an infinite tower of double trace operators, the phase is responsible for the appearance of a singularity, which turns out to be dominated by the large- n tail of the sum [11]. In formulae [40]:

$$z\bar{z}(\bar{z} - z) \mathcal{H}_{\text{Lorentzian}}(z, \bar{z}) \approx -64i\pi \sum_n n^2 e^{2ixn} \sum_{\ell \text{ even}} (\ell + 1)^2 P_\ell(\cos \theta) \frac{\langle a e^{-i\pi\gamma} \rangle_{n, \ell}}{\langle a^{(0)} \rangle_{n, \ell}}, \quad (2.37)$$

where $x \sim z - \bar{z} \rightarrow 0$ parametrizes how to approach the singularity and P_ℓ are four dimensional Legendre polynomials. The left hand side of Eq. (2.37) is the quantity that we are going to relate to the scattering amplitude in the dual gravity theory. In the right hand side instead, we recognize the familiar partial wave expansion valid for amplitudes in generic quantum field theory, thus motivating the following relation:

$$\lim_{n \rightarrow \infty} \frac{\langle a e^{-i\pi\gamma} \rangle_{n, \ell}}{\langle a^{(0)} \rangle_{n, \ell}} = b_\ell(s), \quad L\sqrt{s} = 2n \quad (2.38)$$

where $b_\ell(s)$ are the coefficients of the partial wave expansion of the flat space gravity amplitude, we will come back to them in Sec. 3.

Let us summarize: so far we have seen that to determine the singular behaviour of the CFT correlator in the bulk point regime we need to study averages (over mixing index) of the type $\langle ae^{-i\pi\gamma} \rangle$ in the large n limit. On the gravity side for weakly coupled theories, these singularities correspond to *bulk Landau diagrams* (see [42] for details) which can be computed as in flat space time. Finally, the linking point between CFT and gravity is given by Eq. (2.38).

Given (2.13) and (2.14), the average $\langle ae^{-i\pi\gamma} \rangle$ admits the large c expansion

$$\begin{aligned} \langle ae^{-i\pi\gamma} \rangle_{n,\ell} = & \langle a^{(0)} \rangle + c^{-1} \left(\langle a^{(1)} \rangle - i\pi \langle a^{(0)} \gamma^{(1)} \rangle \right) + c^{-2} \left(\langle a^{(2)} \rangle - i\pi \langle a^{(1)} \gamma^{(1)} + a^{(0)} \gamma^{(2)} \rangle \right. \\ & \left. - \frac{\pi^2}{2} \langle a^{(0)} \gamma^{(1)2} \rangle \right) + c^{-3} \left(\langle a^{(3)} \rangle - i\pi \langle a^{(2)} \gamma^{(1)} + a^{(1)} \gamma^{(2)} + a^{(0)} \gamma^{(3)} \rangle \right. \\ & \left. - \pi^2 \left\langle \frac{a^{(1)} \gamma^{(1)2}}{2} + a^{(0)} \gamma^{(1)} \gamma^{(2)} \right\rangle + \frac{i\pi^3}{6} \langle a^{(0)} \gamma^{(1)3} \rangle \right) + \mathcal{O}(c^{-4}). \end{aligned} \quad (2.39)$$

The large n limit can then be taken using directly the inversion formula and results in an expression depending solely on the dDisc defined above [11],

$$\begin{aligned} \frac{\langle ae^{-i\pi\gamma} \rangle_{n,\ell}}{\langle a^{(0)} \rangle_{n,\ell}} \xrightarrow{n \gg 1} & 1 + \frac{i\pi n^3 c^{-1}}{2(l+1)} + \sum_{\kappa=2} \frac{c^{-\kappa}}{n^2(\ell+1)} \int_C \frac{dx}{2\pi i} e^{-2nx} \\ & \times \int_0^1 \frac{d\bar{z}}{\bar{z}^2} \left(\frac{1 - \sqrt{1 - \bar{z}}}{1 + \sqrt{1 - \bar{z}}} \right)^{l+1} \frac{\text{dDisc} [z\bar{z}(\bar{z} - z)\mathcal{H}^{(\kappa)}(z^\circ, \bar{z})]}{4\pi^2}. \end{aligned} \quad (2.40)$$

Finally the flat space limit is realised by taking $z = \bar{z} + 2x\bar{z}\sqrt{1 - \bar{z}}$ with $x \rightarrow 0$ after having analytically continued z around 0 (z° in the formula above stands exactly for the continuation $z \rightarrow z e^{-2\pi i}$). The x -integral has the effect of converting powers of $\frac{1}{z - \bar{z}}$, which are related to the expansion order κ through (2.26), into powers of n , and consequently of $L\sqrt{s}$ according to Eq. (2.38). Finally in this integral above C is a key-hole contour encircling the origin clockwise.

2.4 Flat space limit of higher logarithmic terms at all loops

The relation (2.40) assumes the knowledge of the full double discontinuity of the correlator, however, as anticipated before, Eq. (2.31) is sufficient to only partially fix it for $\kappa > 2$, thus making impossible to completely use this expression and a direct comparison with the amplitude. However as we have seen explicitly for the $\kappa = 3$ case in [10], which is reviewed in Appendix B.1, something interesting can still be said also for these higher logarithmic terms.

Let us start by taking a closer look at the expression in (2.31): in the $x \rightarrow 0$ limit the dominant terms are the most divergent ones as $z \rightarrow \bar{z}$ (i.e. the highest powers of $\frac{1}{z - \bar{z}}$). This observation greatly simplifies our computation, especially when applying $\mathcal{D}_{(3)}$ in Eq. (2.32)

and $\Delta^{(8)}$ in Eq. (2.27). Indeed the evaluation of Eq. (2.31) reduces to:

$$\{\mathcal{D}_{(3)}h^{(\kappa)}(z) + (z \leftrightarrow \bar{z})\} \xrightarrow{\text{flat space}} \left(\frac{z\bar{z}}{z-\bar{z}}\right)^7 (h^{(\kappa)}(z) - h^{(\kappa)}(\bar{z})) , \quad (2.41)$$

$$[\Delta^{(8)}]^{\kappa-1} \{\mathcal{D}_{(3)}h^{(\kappa)}(z) + (z \leftrightarrow \bar{z})\} \xrightarrow{\text{f.s.}} \frac{7 \cdot 3^{2\kappa-1} 64^{\kappa-1} (z\bar{z})^7}{(z-\bar{z})^{8\kappa-1}} w_\kappa(z, \bar{z}) (h^{(\kappa)}(z) - h^{(\kappa)}(\bar{z})) . \quad (2.42)$$

where in the second line we have divided everything by $(z\bar{z})^2$ to adjust it to our normalization. Notice that the power of $(z-\bar{z})$ correctly reproduces our prediction in Eq. (2.26) ($8\kappa-1 = a+4$). $w_\kappa(z, \bar{z})$ is a polynomial of degree $4(3\kappa-4)$, which, in the limit $z = \bar{z}$ we are working in, reduces to

$$w_\kappa(z, \bar{z}) \xrightarrow{z=\bar{z}} \frac{1}{35} 8^{1-2\kappa} 9^{-\kappa} \Gamma(8\kappa-2) (1-\bar{z})^{4(\kappa-1)} \bar{z}^{4(2\kappa-3)} . \quad (2.43)$$

Putting everything together, one finally finds

$$\begin{aligned} & \frac{\text{dDisc}[z\bar{z}(\bar{z}-z)]\mathcal{H}^{(\kappa)}|_{\log^\kappa(z,\bar{z})}(z^\circ, \bar{z})}{4\pi^2} \xrightarrow{\text{flat space}} \frac{\Gamma[8\kappa-2]}{(2x)^{8\kappa-2}} \frac{(1-\bar{z})^{4\kappa+3}}{120\bar{z}^{4\kappa}} \times \\ & \times \frac{1}{4\pi^2} \text{dDisc} \left[\frac{(z\bar{z})^2}{(1-z)^2(1-\bar{z})^2} \log^\kappa((1-z)(1-\bar{z})) (h^{(\kappa)}(1-z^\circ) - h^{(\kappa)}(1-\bar{z})) \right]_{z=\bar{z}} \\ & \equiv \frac{\text{dDisc}[\log^\kappa((1-\bar{z})(1-z))]_{z=\bar{z}}}{4\pi^2} g^{(\kappa)}(\bar{z}) , \end{aligned} \quad (2.44)$$

where we have explicitly used crossing symmetry to pass to the t -channel. Notice that since one has to take $z = \bar{z}$, the only terms surviving in the difference are the ones coming from the analytic continuation of z around the origin. Moreover, given that only integer powers of $(1-\bar{z})$ appear and $h^{(\kappa)}$ can not contain $\log(1-\bar{z})$, dDisc acts non trivially only on $\log^\kappa(1-\bar{z})$, thus returning Eq. (2.34). The last point that we want to stress is that, as it is evident from (2.44), in the flat space limit we do not have to take any derivatives, streamlining a lot the computations and eventually the only information one needs to know is an explicit expression for the $h^{(\kappa)}$'s. Eq. (2.33) gives a very compact prescription for finding them, but it involves an infinite sum, which is not straightforward to solve. Quite remarkably, we have found a simple algorithm to compute this quantity, allowing us to study different cases⁶ and deduce a general form at any order in c .

First of all we have noticed the general structure

$$\begin{aligned} h^{(\kappa)}(z) = & j_0(z) + j_1(z)H_1(z) + \left(j_2(z)K_2(z) + j_2\left(\frac{z}{z-1}\right)I_2(z) \right) \\ & + \left(j_3\left(\frac{z}{z-1}\right)K_3(z) + j_3(z)I_3(z) \right) + \dots + \begin{cases} (j_\kappa(z)K_\kappa(z) + j_\kappa\left(\frac{z}{z-1}\right)I_\kappa(z)) & \text{for } \kappa \text{ even} \\ (j_\kappa\left(\frac{z}{z-1}\right)K_\kappa(z) + j_\kappa(z)I_\kappa(z)) & \text{for } \kappa \text{ odd} \end{cases} \end{aligned} \quad (2.45)$$

⁶We have computed the full form of $h^{(\kappa)}$ up to $\kappa = 7$, their expressions can be found in the ancillary Mathematica file, and for the highest transcendental pieces up to $\kappa = 21$.

where j_i are generic function, I_n and K_n are iterative integrals defined as

$$I_n(z) = \int_0^z \frac{dz'}{z'(1-z')^{(n-1)\bmod 2}} I_{n-1}(z') \quad \text{where} \quad I_1(z) \equiv H_1(z), \quad (2.46)$$

$$K_n(z) = \int_0^z \frac{dz'}{z'(1-z')^{n\bmod 2}} K_{n-1}(z') \quad \text{where} \quad K_1(z) \equiv H_1(z). \quad (2.47)$$

Here and in the following we will denote with $H_{\dots}(x)$ the Harmonic Polylogarithms (HPL), which are defined in Appendix A. It follows directly from their definition that, both for the I and K integral, at each step n we are adding alternatively a 0 or a 0 and a 1 to each HPL appearing at order $n-1$, i.e. $H_{a_1\dots a_{n-1}}(z) \rightarrow H_{0a_1\dots a_{n-1}}(z)$ or $H_{a_1\dots a_{n-1}}(z) \rightarrow H_{0a_1\dots a_{n-1}}(z) + H_{1a_1\dots a_{n-1}}(z)$. Hence, starting from $H_1(z)$, a one is always followed by a zero and there are no two consecutive ones to the left of the index vector; the only exception is $H_{11}(z)$ in I_2 . This is enough to state that the maximal logarithmic divergence⁷ of $\sim \log(1-z)$ -type that $h^{(\kappa)}$ can develop is precisely $H_{11}(z)$ and this term produces a $\log^2 V$ in the small V expansion of the correlator. The full leading logarithmic term will eventually inherit the same behaviour, even away from the flat space limit, so we expect

$$\text{leading logs in } \mathcal{H}^{(\kappa)} \sim \log^\kappa U \log^2 V. \quad (2.48)$$

In this way we have explicitly checked to all order the conjectures in [10], which was originally inspired by a diagrammatic interpretation in the dual gravity theory, see also [45].

To conclude, from the study of different explicit examples we are able to find a close expression for the two highest transcendentality terms in (2.45),

$$\begin{cases} p_\kappa(z)K_\kappa(z) + p_\kappa\left(\frac{z}{z-1}\right)I_\kappa(z) + q_\kappa\left(\frac{z}{z-1}\right)K_{\kappa-1}(z) + q_\kappa(z)I_{\kappa-1}(z) & \kappa \text{ even} \\ p_\kappa\left(\frac{z}{z-1}\right)K_\kappa(z) + p_\kappa(z)I_\kappa(z) + q_\kappa(z)K_{\kappa-1}(z) + q_\kappa\left(\frac{z}{z-1}\right)I_{\kappa-1}(z) & \kappa \text{ odd} \end{cases} \quad (2.49)$$

where the polynomials are defined as

$$p_\kappa(z) = \frac{(-1)^\kappa 4^{3-2\kappa} 15^{1-\kappa}}{z^5 \kappa!} \left((-6 \cdot 5^\kappa + 10^\kappa + 50) z^2 + 3(5^\kappa - 25) z + 30 \right), \quad (2.50)$$

$$\begin{aligned} q_\kappa(z) = \frac{\left(-\frac{1}{3}\right)^\kappa 2^{4-4\kappa} 5^{1-\kappa}}{z^5 \kappa!} \{ & -12(-3 \cdot 5^\kappa + 10^\kappa + 5) z^4 + (-54 \cdot 5^\kappa + 3 \cdot 10^{\kappa+1} - 30) z^3 \\ & + (6(17 \cdot 5^\kappa + 10^\kappa + 265) - 2(39 \cdot 5^\kappa + 2^{\kappa+1} 5^\kappa + 685) \kappa) z^2 \\ & + (3(13 \cdot 5^\kappa + 685) \kappa - 60(5^\kappa + 43)) z + 1104 - 822\kappa \}. \end{aligned} \quad (2.51)$$

In Appendix C we find the same polynomials starting this time from the amplitude and we will explain how to connect the results from both sides⁸.

⁷Remember that $h^{(\kappa)}$ does not contain $\log z$ because by definition they are already factored out in the correlation function.

⁸For the highest transcendental term an expression was found also in [12] and it matches the one we obtained.

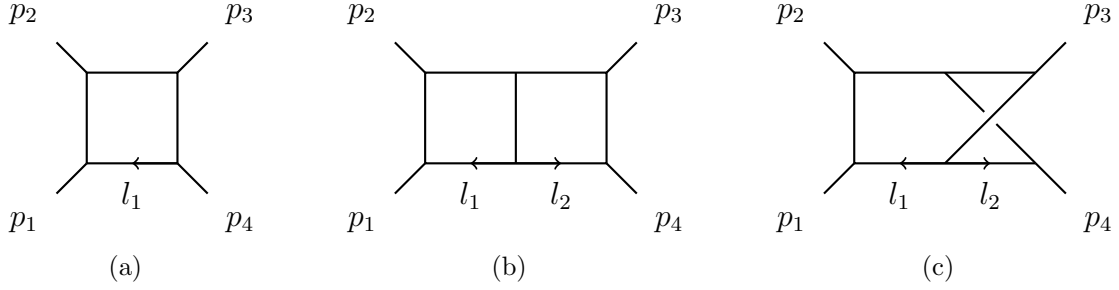


Figure 2: One loop planar box digram (a) and two loop planar (a) and non planar (b) double box diagram.

3 Four-graviton scattering amplitude

It is well known that $\frac{1}{N}$ corrections to the four point functions of four \mathcal{O}_2 half-BPS operators in $\mathcal{N} = 4$ SYM in the $\lambda \rightarrow \infty$ limit are dual to perturbative scattering amplitudes of gravitons in IIB supergravity on $\text{AdS}_5 \times \text{S}^5$. For the purposes of studying the CFT bulk-point limit, the background geometry can be effectively taken to be ten dimensional flat space, so that the final object we are going to study is \mathcal{A}_{10}^{sugra} , denoting the supergravity amplitude of four gravitons in \mathbb{R}^{10} . Similarly to the $1/c$ expansion in Eq. (2.10), this quantity admits a loop expansion in powers of the gravitational constant G_N and up to two loops this reads

$$\begin{aligned}
\mathcal{A}_{10}^{sugra} &= \hat{K} \left\{ \frac{8\pi G_N}{stu} + (8\pi G_N)^2 (I_{box}(s, t) + I_{box}(s, u) + I_{box}(t, u)) \right. \\
&+ (8\pi G_N)^3 \left(s^2 \left(I_{db}^{pl}(s, t) + I_{db}^{np}(s, t) + t \leftrightarrow u \right) + t^2 \left(I_{db}^{pl}(t, s) + I_{db}^{np}(t, s) + s \leftrightarrow u \right) \right. \\
&\left. \left. + u^2 \left(I_{db}^{pl}(u, s) + I_{db}^{np}(u, s) + s \leftrightarrow t \right) \right) + \mathcal{O}(G_N^4) \right\} \\
&\equiv (\pi L)^5 s^4 \left\{ \frac{L^3 F_1(x)}{s^3 c} + \frac{L^{11} s F_2(x)}{c^2} + \frac{L^{19} s^5 F_3(x)}{c^3} + \mathcal{O}(c^{-4}) \right\}, \tag{3.1}
\end{aligned}$$

where we have reported the value of the amplitude at tree-level, while at higher loops we have substituted it with the sum of the corresponding Feynman diagrams. Here I_{box} , I_{db}^{pl} and I_{db}^{np} indicate respectively the one-loop box diagram, planar and non planar double box in Fig. 2. With s, t and u we denote the usual Mandelstam variables satisfying the constraint $s+t+u=0$. \hat{K} is a dimension-eight kinematic factor, depending on the polarizations of the gravitons. In order to compare the amplitude with $\mathcal{G}(U, V)$, these polarization vectors should be chosen to be null tensors and orthogonal to all the external momenta; in this configuration \hat{K} reduces to an overall s^4 factor. In the second line we have used the identification $8\pi G_N = \pi^5 L^8 c^{-1}$ to make manifest the relation with the large c expansion with $L = L_{\text{AdS}_5} = L_{\text{S}^5}$ the AdS and sphere radii. The F_κ are functions of the adimensional parameter $-\frac{t}{s} = 1 - x = \frac{1 - \cos\theta}{2}$, which has been introduced to make the s and L dependence manifest. These factors are in fact the ones related to the large n behaviour of the correlator, as prescribed by Eq. (2.38).

The five dimensional \mathcal{A}_5 amplitude is obtained by dividing \mathcal{A}_{10}^{sugra} by the sphere volume

$\pi^3 L^5$ and it can be expanded in partial waves as

$$i\mathcal{A}_5(s, t) = \frac{128\pi}{\sqrt{s}} \sum_{\ell \text{ even}} (\ell + 1)^2 b_\ell(s) P_\ell(\cos \theta). \quad (3.3)$$

Using the orthonormality of the Legendre polynomials, one can extract the coefficients as

$$\begin{aligned} b_\ell(s) &= 1 + \frac{i\pi}{\ell + 1} \int_0^\pi \frac{d\theta}{\pi} \sin \theta \sin((\ell + 1)\theta) \frac{\sqrt{s}\mathcal{A}_5(s, \cos \theta)}{64\pi^2} \\ &= 1 + \left(\frac{L\sqrt{s}}{2}\right)^3 \frac{i\pi c^{-1}}{2(\ell + 1)} + \sum_{\kappa=2} \frac{2\pi i c^{-\kappa}}{\ell + 1} \int_0^1 \frac{d\bar{z}}{\bar{z}^2} \left(\frac{1 - \sqrt{1 - \bar{z}}}{1 + \sqrt{1 - \bar{z}}}\right)^{\ell+1} \\ &\quad \times (\text{disc}_t + (-1)^\ell \text{disc}_u) \frac{\sqrt{s}\mathcal{A}_5^{(\kappa)}(s, \cos \theta)}{64\pi^2}, \end{aligned} \quad (3.4)$$

where we have defined $\mathcal{A}_5^{(\kappa)}$ as the $(\kappa - 1)$ -loop amplitude. In the second line we have plugged in the explicit expression for \mathcal{A}_5^{tree} , while for the other orders we have expressed the amplitude through its discontinuities via a dispersion relation [11, 44]. In the cases at hand, ℓ runs over even integers, so that the discontinuity in the t -channel (disc_t) and the one in the u -channel (disc_u), taken at fixed s , actually sum up.

The expressions in Eq. (3.3) and (3.4) are very reminiscent of Eq. (2.37) and (2.40), thus motivating the following identifications:

$$\frac{\langle a e^{-i\pi\gamma} \rangle_{n,\ell}}{\langle a^{(0)} \rangle_{n,\ell}} \xrightarrow{n \rightarrow \infty} b_\ell(s), \quad (3.5)$$

$$\text{dDisc}[\mathcal{H}(z, \bar{z})] \xrightarrow{\text{flat space}} \text{disc}\mathcal{A}_5. \quad (3.6)$$

Once again, these relations apply to the full double discontinuity and have been proven to be exact at order $\kappa = 2$.

3.1 The two loop example as the starting point

While we collect all the details for the $\kappa = 3$ case in Appendix B.2 and B.3, here we would like to briefly discuss its most relevant features, since this example clearly illustrates the two main points that will characterize the higher loop generalization, namely *the appearance of multi-trace operators* in the OPE and the relation between leading logarithms and *iterated s -cuts*.

Up to two loops, Eq. (2.40) reads

$$\begin{aligned} \frac{\langle a e^{-i\pi\gamma} \rangle_{n,\ell}}{\langle a^{(0)} \rangle_{n,\ell}} &\rightarrow 1 + \frac{i\pi n^3}{2c(\ell + 1)} + \frac{i\pi}{\ell + 1} \int_0^1 \frac{d\bar{z}}{\bar{z}^2} \left(\frac{1 - \sqrt{1 - \bar{z}}}{1 + \sqrt{1 - \bar{z}}}\right)^{\ell+1} \times \\ &\quad \left\{ \frac{n^{11}}{c^2} g^{(2)}(\bar{z}) + \frac{n^{19}}{c^3} \left(\log(1 - \bar{z}) g^{(3)}(\bar{z}) + \underbrace{\dots}_{\text{from } \log^2 U} \right) + \mathcal{O}\left(\frac{n^{8\kappa-5}}{c^\kappa}\right) \right\}, \end{aligned} \quad (3.7)$$

where $g^{(2)}(\bar{z})$ is given in Eq. (5.22) of [11] and the dots represent the pieces in the $\mathcal{H}^{(3)}$ correlator multiplying $\log^2(z\bar{z})$. The latter terms contribute to the dDisc, but unfortunately we do not have an expression for them. There are both technical and conceptual problems to compute these terms, just to mention few of them, higher trace operators appear in the OPE and contribute to the dDisc and the mixing problem needs to be solved at a higher N order (e.g. $\gamma_{n,\ell,I}^{(2)}$ needs to be computed).

On the supergravity side we have that (3.4) reduces to

$$b_\ell(s) = 1 + \left(\frac{L\sqrt{s}}{2}\right)^3 \frac{i\pi}{2c(\ell+1)} + \frac{i\pi}{\ell+1} \int_0^1 \frac{d\bar{z}}{\bar{z}^2} \left(\frac{1-\sqrt{1-\bar{z}}}{1+\sqrt{1-\bar{z}}}\right)^{\ell+1} \times \quad (3.8)$$

$$\left\{ \left(\frac{L\sqrt{s}}{2}\right)^{11} \frac{1}{c^2} g_2(\bar{z}) + \left(\frac{L\sqrt{s}}{2}\right)^{19} \frac{1}{c^3} \text{disc}_{x>1} F_3(x) \Big|_{x=\frac{1}{\bar{z}}} + \mathcal{O}\left(\left(\frac{L\sqrt{s}}{2}\right)^\kappa c^{-\kappa}\right) \right\},$$

where

$$\text{disc}_{x>1} F_3(x) \equiv \frac{1}{2\pi i} (F_3(x+i0) - F_3(x-i0)). \quad (3.9)$$

Comparing the two results, the first thing we notice is that given the form of $\text{dDisc}\mathcal{H}^{(3)}|_{\log^3 z\bar{z}}$, only the planar diagrams contribute. The finite part of the non-planar one, in fact, has a completely different structure: the highest transcendental weight⁹ is three and consequently two for the discontinuity. As we are interested in matching the highest logarithmic part and this contribution is subleading, we can discard it in the comparison with the CFT. We believe that the non planar contributions will appear in the $\log^2 U$ and lower terms of the four-point correlator. Even when restricting to I_{ab}^{pl} , Eqs. (3.7) and (3.8) do not agree completely. To investigate the motivation behind this mismatch, we decided to get back to the definition of a discontinuity and its interpretation in terms of *unitarity cuts*.

It is known [46] that the s -channel discontinuity of a generic amplitude \mathcal{A} , $\text{disc}_s \mathcal{A}$, is given by the sum over all possible cuts where s is the momentum flowing. A given cut diagram can be constructed from the integral representation by putting on-shell the cut propagators. In our case¹⁰, this translates diagrammatically in

$$2\pi i \text{disc}_s \mathcal{A} = \underbrace{\text{diagram}_1 + \text{diagram}_2}_{c_1} + \underbrace{\text{diagram}_3 + \text{diagram}_4}_{c_2}. \quad (3.10)$$

From this picture we can clearly separate two types of contributions and we can try to reinterpret them from the CFT point of view, similarly as done in [10, 23].

We argue that the first type of cut (c_1) translates the double trace operator exchange, the only one that we have information about, while the second one (c_2) corresponds to

⁹Here and in the following we will consider as “highest transcendental weight” those functions that have the highest transcendental weight and with a non vanishing discontinuity, thus disregarding constant such as powers of π or ζ_n .

¹⁰At two loop and restricting F_3 to the planar contributions only, $\text{disc}_s \mathcal{A} = -\text{disc}_{x>1} F_3(x)$.

the exchange of triple trace operators. The two contributions can be computed separately, thus allowing us to compare each of them with the CFT. Naively one can think that c_1 should reproduce $g^{(3)}$ since we have concretely disentangled the triple trace contributions, however that is not the case. In fact, we have to remember that the conjecture connects the discontinuity of the amplitude, and relatedly c_1 , with the entire dDisc and we are missing $\log^2 U$ term in the correlator. So we have to carefully rethink the results that we obtain when considering the double discontinuity of the $\log^3 U$ term and interpret them from a different perspective. We know that when computing $\mathcal{H}^{(3)}|_{\log^3(z\bar{z})}$ we are taking the product of three tree-level anomalous dimensions $\gamma^{(1)}$, so the question one should ask is: what is the analogue of this quantity on the amplitude side?

In perturbative quantum field theory, one can compute the imaginary part of an amplitude at a generic loop L knowing the results at lower loops, namely up to $(L - 1)$. Similar unitarity methods hold in CFT, see [1, 23, 24] for example, where instead of integrating over the phase space of the intermediate states, as one usually does for amplitudes, one has to sum over all the states exchanged in the OPE of the correlator. Reinterpreted from this perspective, at two loops it was naive to expect that the results from c_1 , which knows intrinsically about one loop information, would have matched exactly the dDisc of the higher logarithmic part of the correlator, constructed from $(\gamma^{(1)})^3$. So to make a sensible comparison, one should look for a different object built from the amplitude and depending only on tree-level “two-particles” data. In [10], we found that such an object exists and that the CFT contribution we have computed is proportional to a saturated s -channel cut, a diagram with all the possible s -cuts passing only through two propagators. At this loop order, we call this quantity *double cut*, c_{dc} . Remarkably we find a perfect agreement, i.e.



$$= 32s^5 g^{(3)}(\bar{z}) \quad (3.11)$$

with $g^{(3)}(\bar{z})$ as defined in Eq. (B.8), where the matching is also with all the numerical factors.

3.2 Higher Loop generalisation

In the spirit of understanding more and more how unitarity methods which are valid for S-matrix elements can be applied in the CFT context, we would like to extend the validity of this iterated s -cut construction to all loops and eventually compare these results with the ones in Sec. 2.4. Even if our analysis will be restricted to flat space, similar arguments should remain valid for the full $\text{AdS}_5 \times \text{S}^5$ amplitude, thus possibly shedding some light on potential structures appearing there and how to extract them.

To actually compute this iterated cut, one can think of generalizing the differential equation method we have been using for $\kappa = 3$ to higher loops. However this becomes computationally hard already at three loops and at higher order it is not possible to find a way to a priori fix the needed boundary conditions. An alternative approach is thus necessary. Before illustrating it, let us comment that despite the possible appearance of higher order divergences as κ increases, it has been known for a while and largely used in the literature that the iterated two-particle cut is actually finite to all orders [47], as we have explicitly seen at two loops.

Let us start by going back to the general definition of a cut: a given cut diagram is a Feynman diagram in which the cut propagators are put on-shell. In the related integral, this corresponds to replace $\frac{1}{p^2-m^2+i\epsilon}$ with $-2\pi i\delta^{(+)}(p^2-m^2)$, a one-dimensional delta function of the same argument, for each cut propagator. For example, in the one loop case, we have

$$\text{Diagram} \propto \int d^D k_1 \frac{\delta^{(+)}(k_1^2)\delta^{+}((k_1-p_1-p_2)^2)}{(k_1-p_1)^2(k_1+p_4)^2}, \quad (3.12)$$

where k_1 represents the loop momentum. Generalized to $(\kappa-1)$ loop, the iterated s -channel cut for the κ rungs ladder diagram takes the form

$$\text{Diagram} \propto \int \prod_{i=1}^{\kappa-1} d^D k_i \frac{\delta^{+}(q_1^2)\delta^{+}(q_2^2)\cdots\delta^{+}(q_{2\kappa-2}^2)}{q_{2\kappa-1}^2\cdots q_{3\kappa-2}^2}, \quad (3.13)$$

where q_i^μ is a combination of external and loop momenta k_i^μ . Thus another way to compute the iterated s -channel cut is to solve directly this integral. Before continuing with the details of the computation, let us set some notation: we are working in Lorentzian signature ($\text{diag}(1, -1, \dots)$), in our conventions all the D -dimensional external momenta are outgoing and in the centre of mass frame they take the following form

$$p_1^\mu = \frac{1}{2\sqrt{s}}\{1, 1, \vec{0}_{D-2}\}, \quad p_2^\mu = \frac{1}{2\sqrt{s}}\{1, -1, \vec{0}_{D-2}\}, \quad p_4^\mu = \frac{1}{2\sqrt{s}}\{-1, -\cos\chi, -\sin\chi, \vec{0}_{D-3}\}.$$

Energy-momentum conservation fixes $p_1^\mu + p_2^\mu + p_3^\mu + p_4^\mu = 0$. The loop momenta can be parametrized as

$$k_1^\mu = \frac{1}{2\sqrt{s}}\{E_{k_1}, |k_1|\cos\theta_1, |k_1|\sin\theta_1\cos\theta_2, |k_1|\sin\theta_1\sin\theta_2, \vec{0}_{D-4}\}, \quad (3.14)$$

and the corresponding measure

$$\int d^D k_1 \propto \int dE_{k_1} \int d|k_1| |k_1|^{\frac{D-1}{2}} \int_0^{2\pi} d\theta_2 \sin^{D-4}\theta_2 \int_0^\pi d\theta_1 \sin^{D-3}\theta_1. \quad (3.15)$$

From now on we will fix D to be 10 and we will start by computing the s -cut of the one loop box integral in Eq. (3.12). The two delta functions can be used to perform the integration in E_{k_1} and $|k_1|$, such that the loop momentum reduces to

$$k_1^{\mu OS} = \frac{1}{2\sqrt{s}}\{1, \cos\theta_1, \sin\theta_1\cos\theta_2, \sin\theta_1\sin\theta_2, \vec{0}_{D-4}\}. \quad (3.16)$$

After this simplification, the integral (3.12) becomes¹¹

$$\int \underbrace{d\theta_2 d\theta_1 \sin^6\theta_2 \sin^7\theta_1}_{\text{measure}} \underbrace{\frac{1}{s^2(1-\cos\theta_1)}}_{I_{\text{left}}} \times \underbrace{\frac{1}{(1-\cos\chi\sin\theta_1-\cos\theta_2\sin\chi\sin\theta_1)}}_{I_{\text{right}}}, \quad (3.17)$$

¹¹Similar results were already know in the literature, see for example Appendix A of [48]. AG thanks S. Abreu for pointing out this reference.

where we have suppressed some numerical factors for simplicity and beside the measure, we can distinguish two pieces: a left and a right integrand. The θ_2 integration can be done straightforwardly, then we can perform a simple change of variable, $\cos \theta_1 = 2v - 1$, to express the remaining integral as one in v ranging from 0 to 1. To make contact with the usual expressions in terms of Mandelstam invariants, we can identify $\cos \chi = \frac{s+2t}{s}$. The integrand then takes the form

$$\begin{aligned} & \frac{\pi}{2st^3(v-1)(s+t)^3} (-s(s+t-sv))^4 \left| \frac{t}{s} - v + 1 \right| + (s+t)^5 - 5sv(s+t)^4 \\ & + 10s^2v^2(s+t)^3 - 10v^3(s+t)^2 (s^3 + 2t^3) + 5v^4(s+t) (s^4 + 8st^3 + 6t^4) \\ & + v^5 (-20s^2t^3 - s^5 - 30st^4 - 12t^5) \equiv \frac{\mathcal{K}(v, s, t)}{2s(1-v)}. \end{aligned} \quad (3.18)$$

The absolute value comes from the square roots appearing after the θ_2 integration and as a consequence of their presence the integration region is split in two subsets: v less or greater than $\frac{s+t}{s}$ (where we are considering $s < 0$). The last integration then gives

$$\mathcal{R}_1(s, t) = \text{[Diagram: a square with a vertical dashed red line through its center]} \propto \int_0^{\frac{t+s}{s}} dv \frac{\mathcal{K}^+(v, s, t)}{2s(1-v)} + \int_{\frac{t+s}{s}}^1 dv \frac{\mathcal{K}^-(v, s, t)}{2s(1-v)}, \quad (3.19)$$

where we have defined

$$\mathcal{K}^\pm = \mathcal{K}|_{|x|=\pm x}. \quad (3.20)$$

This matches the result of [11] up to an overall factor which comes from normalization.

The uptake of this construction is that it can be easily generalized to higher loops. Similarly to the box integral which was constructed integrating over the product of the two pieces in Eq. (3.17) separated by the cut, we can now glue the same right integrand to the one-loop result to construct the two-loop case. Then the idea is that to compute the L -loop integral, we can keep on multiplying the right integrand in Eq. (3.17) for the result obtained at order $(L-1)$.

Let us start from the two-loop case and let us see how we can retrieve the result in Sec. 3.1 for the *double cut*. Notice that the left integrand in Eq. (3.17) has no θ_2 dependence, so we can directly take the integrated result (3.18) and multiply it by the left integrand, i.e. $2s(1-v)$, to obtain the needed kernel $\mathcal{K}(v, s, t)$. Consequently, at two loops we get

$$\text{[Diagram: a square with two vertical dashed red lines through its center]} \propto \int_0^{\frac{t+s}{s}} dv \mathcal{R}_1(s, -s(1-v)) \mathcal{K}^+(v, s, t) + \int_{\frac{t+s}{s}}^1 dv \mathcal{R}_1(s, -s(1-v)) \mathcal{K}^-(v, s, t), \quad (3.21)$$

where the new definition of t comes from the fact that the leg associated to p_4^μ is now $k_1^{\mu OS}$. This result matches both with the CFT $g^{(3)}(\bar{z})$ in Eq. (B.8) and with the cut constructions made using differential equations. With respect to the latter, the computation presented here has the advantage of being faster and more efficient as it does not require the knowledge of a canonical basis or integral by parts identities.

As an aside comment, let us mention that at two loop we can obtain c_1 through a similar

construction, the only difference is that now we have to use one-loop integral as the right integrand. To be more precise,

$$\text{Diagram} \propto \int_0^{\frac{t+s}{s}} dv \text{Diagram}^+ \mathcal{K}^+(v, s, t) + \int_{\frac{t+s}{s}}^1 dv \text{Diagram}^- \mathcal{K}^-(v, s, t), \quad (3.22)$$

where again we have redefined t to be $-s(1-v)$. Also in this case the integration is finite, as the c_1 divergence comes only from the box contribution. For this reason we have to compute the kernel $\mathcal{K}(v, s, t)$ up to order ϵ to obtain the finite part of the result. Fortunately this can be done, it is sufficient to perform the θ_2 integration in d -dimension, which gives us a more involved result containing ${}_2F_1$ functions, and then expand the result up to the required order.

As anticipated before, the procedure yielding to Eq. (3.21) can be easily extended to all loops as

$$\mathcal{R}_L(s, t) = \int_0^{\frac{t+s}{s}} dv \mathcal{R}_{L-1}(s, -s(1-v)) \mathcal{K}^+(v, s, t) + \int_{\frac{t+s}{s}}^1 dv \mathcal{R}_{L-1}(s, -s(1-v)) \mathcal{K}^-(v, s, t). \quad (3.23)$$

With these results at hand we can now finally compare them with the ones obtained in Sec. 2.4: we find matches up to 20-loops for the highest weight coefficients (see Appendix C) and up to 6-loops for the full answer. This is a highly non trivial check of the method presented above and of our conjecture relating the dDisc of leading logarithmic terms in the correlator, up to a log factorization¹², and iterated s -channel cuts of the amplitude. Pictorially this translates in

$$\text{Diagram} \propto g^{(\kappa)}(\bar{z}) \quad (3.24)$$

where $g^{(\kappa)}(\bar{z})$ is defined in Eq. (2.44).

Interestingly the same approach can be in principle used in any dimension, except 4 where the interested integral is actually divergent.

Before concluding, let us mention that this identification can also be interpreted as an a posteriori justification for our choice of focusing only on planar ladder diagrams when dealing with CFT leading logarithm terms. These diagrams are indeed the only ones presenting exactly $(\kappa-1)$ iterated two-particle cuts and as a consequence containing the same information as in the CFT leading log pieces. In going to higher order one should be more careful on the type of integrands appearing in the amplitude and the associated Feynman diagrams but we believe that all other diagrams apart from planar ladders should map to different $\log^k U \log^j V$, with k strictly less than κ . For example at three loops we believe that

$$\text{Diagram} \approx \log^3(U) \log^3(V) \quad (3.25)$$

¹²To have an exact match between iterated cuts and CFT correlator in the flat space limit without any log factorization, one can consider instead of the double discontinuity some sort of $\underbrace{\text{d} \dots \text{d}}_{\kappa-1} \text{Disc}$, such that it returns directly $g^{(\kappa)}(\bar{z})$.

Having a complete understanding of higher loops contributions enabling us to check our intuitions, would also require the knowledge of the unmixed OPE data starting already from the ones at order c^{-1} . This represents a very challenging problem, so for the moment our discussion for $\kappa \geq 4$ should be taken as a collection of qualitative observations based on explicit examples. We plan nonetheless to give a more concrete answer to these problems in the future.

4 Mellin space

There are certain circumstances, such as in the direct comparison with a gravity amplitude, in which certain properties and characteristics become more visible and accessible when considering the Mellin representation of CFT correlators. In this section we will reinterpret our previous results from this prospective in an attempt to understand more deeply the physics in the flat space limit.

4.1 Generalities and flat space limit

In Mellin space $\mathcal{H}(U, V)$ is defined through the integral [49–51]

$$\mathcal{H}(U, V) = \int_{-i\infty}^{i\infty} \frac{ds dt}{(4\pi i)^2} U^{s/2} V^{(t-4)/2} \widetilde{\mathcal{M}}(s, t) \Gamma\left(\frac{4-s}{2}\right)^2 \Gamma\left(\frac{4-t}{2}\right)^2 \Gamma\left(\frac{4-u}{2}\right)^2, \quad (4.1)$$

where s , t and u are dependent variables, very reminiscent of Mandelstam ones, satisfying the constraint $s + t + u = 4$ and $\widetilde{\mathcal{M}}(s, t)$ is the (*reduced*) *Mellin Amplitude*. In this language, the crossing equations (2.12) translates into

$$\widetilde{\mathcal{M}}(s, t) = \widetilde{\mathcal{M}}(t, s). \quad (4.2)$$

The Mellin amplitude inherits from the correlator in the supergravity limit a loop expansion around large c . A term in $\mathcal{H}^{(\kappa)}(U, V)$ that behaves as $\sim \log^k U \log^j V$ would be generated in Mellin space from an infinite sum over simultaneous poles in s and t of the form $\sum_{m,n} \nu_{mn} (s - 2m)^{-k+1} (t - 2n)^{-j+1}$. In particular it has been shown in [15] that at one loop

$$\widetilde{\mathcal{M}}^{(2)}(s, t) = \sum_{m,n=2}^{\infty} \left(\frac{c_{mn}^{(2)}}{(s-2m)(t-2n)} + \frac{c_{mn}^{(2)}}{(t-2m)(u-2n)} + \frac{c_{mn}^{(2)}}{(u-2m)(s-2n)} \right) \quad (4.3)$$

it is sufficient to successfully reproduce the entire $\mathcal{H}^{(2)}(U, V)$, without the addition of any other simple pole or regular term.

The Mellin space formalism turns out to be mostly suited when studying scattering amplitudes. In fact, it has been argued in [52–54] that scattering amplitudes in AdS are Mellin transform of CFT correlators and that in the large s, t limit $\widetilde{\mathcal{M}}(s, t)$ recovers exactly the amplitude computed in flat space-time. The prescription to take this flat space limit, or equivalently large AdS radius, is [13, 55]

$$\lim_{L \rightarrow \infty} L^{14} \pi^3 \frac{\Theta_4^{flat}(s, t, \sigma, \tau)}{16} \widetilde{\mathcal{M}}(L^2 s, L^2 t) = \int_0^\infty d\beta \beta e^{-\beta} \mathcal{A}_{10}^\perp(2\beta s, 2\beta t, \sigma, \tau), \quad (4.4)$$

where σ and τ are the $SU(4)_R$ cross-ratios in Eq. (2.4) and $\Theta_4^{flat}(s, t, \sigma, \tau) \equiv (tu + t\sigma + su\tau)^2$, see [13] and references therein for more details on the derivation of this formula. With \mathcal{A}_{10}^\perp we denote the ten dimensional flat space graviton amplitude in the transverse kinematics: the momenta k_i lie on $\mathbb{R}^5 \simeq \text{AdS}_5|_{L \rightarrow \infty}$ and are orthogonal to the S^5 polarization vectors ($k_1 \cdot y_i = 0$). In this configuration \mathcal{A}_{10}^\perp coincides with \mathcal{A}_{10}^{sugra} in Eq. (3.1) with $\hat{K} = 64 \Theta_4^{flat}(s, t, \sigma, \tau) c(2) \beta^4$ and $c(2) = 1/32\pi^2$.

4.2 Two loops and beyond

Given the behaviour of $\mathcal{H}^{(\kappa)}|_{\log^\kappa(z\bar{z})}$ in Eq. (2.48), for the corresponding Mellin amplitude we consider

$$\widetilde{\mathcal{M}}_{\log}^{(\kappa)}(s, t) = \sum_{m, n=2}^{\infty} \frac{c_{mn}^{(\kappa)}}{(s-2m)^{\kappa-1}(t-2n)}, \quad (4.5)$$

where the subscript log reminds us that we are restricting to the leading logarithmic terms of the correlation function and where we have reported only one channel, all possible cyclic permutations have to be taken into account to get the full amplitude.

The explicit analysis at two loops, whose details can be found in Appendix B.4, has allowed us to formulate the following observations.

- The residue integral associated to the terms in Eq. (4.5) produces not only $\log^\kappa U \log^2 V$ contributions but also lower log powers. For the case $\kappa = 3$ for instance,

$$\begin{aligned} \mathcal{H}^{(3)}(U, V) = & \sum_{m, n=2}^{\infty} \frac{(n-1)_{m+1}^2 c_{mn}}{24\Gamma(m-1)^2} U^m V^{n-2} \log^3 U \log^2 V + \\ & \frac{(n-1)_{m+1}^2 c_{mn}}{4\Gamma(m-1)^2} U^m V^{n-2} (H_{m+n-1} - H_{m-2}) \log^2 U \log^2 V + \dots \end{aligned} \quad (4.6)$$

where $H_l \equiv \sum_{j=1}^l \frac{1}{j}$ represents the Harmonic number. The dots represent contributions from lower powers of $\log U$, $\log V$ terms and from the other pieces of the correlator that we do not know explicitly.

From this expression, it seems that the knowledge of $\sim s^{1-\kappa} t^{-1}$ terms allow to infer something about lower order poles. A deeper understanding of this interplay may give further insight on the full structure of the four-point function. This observation can be related to a similar effect that appears in the flat-space amplitude, where we can indeed reconstruct, up to terms that vanish after iterated discontinuities, the full double trace contribution.

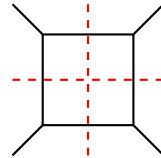
- Now specifying to the two-loop case, in order to get exactly $\mathcal{H}^{(3)}|_{\log^3(z\bar{z})}(U, V)$, we have to consider

$$\sum_{m, n=2}^{\infty} \left(\frac{c_{mn}}{(s-2m)^2(t-2n)} + \frac{c_{mn}}{(s-2m)^2(u-2n)} \right). \quad (4.7)$$

Notice that analogously to what happens in the one-loop case, there is no need to add any $\frac{1}{(s-2m)^2}$ pole. The other permutations appearing in $\widetilde{\mathcal{M}}_{\log}^{(3)}(s, t)$, with m and n properly recombined, give crossing symmetric versions of the correlator. This last fact is in accordance with the discussion in Appendix B.3, where the dDisc of (B.6) is compared with only one channel of the amplitude.

- The flat space limit of $\widetilde{\mathcal{M}}_{\log}^{(3)}(s, t)$, concretely implemented taking $s, t \rightarrow \infty$ with m and n of the same order and carefully regularizing the resulting sum, surprisingly produces a $c_{mn}^{(3)}$ with the same polynomial structure as the one appearing in $I_{db}^{pl}(s, t)$ in Eq. (B.11). However the functions multiplying these polynomials do not have the right transcendental weight to exactly reproduce the space-time amplitude.
- If one further studies the relations between the Mellin result and c_1 and c_2 in Sec. 3.1, it seems to exist a connection between logarithmic singularities, and consequently inverse powers of $(s - 2m)$ and $(t - 2n)$, and discontinuities, corroborating the intuition we have been following throughout the paper.

These observations, together with the identification of leading logs with iterated s -cuts, suggested us that the $c_{mn}^{(\kappa)}$'s should have an interpretation in terms of unitarity cuts. Driven by this intuition, we get back to the easiest example, namely the one-loop Mellin amplitude in its flat space limit. To get it, we need to take m, n large and of order $\mathcal{O}(s, t)$, in this regime the sums become integrals and if we ignore for a second that these sums are divergent, this formula is very reminiscent of the Mandelstam representation for amplitudes¹³ [25, 56]. Hence, it is tempting to compare the $c_{mn}^{(2)}$ with $\text{disc}_s \text{disc}_t I_{box}(s, t)$ and indeed one obtains



$$\propto c_{mn}^{(2)} \Big|_{m=\frac{s}{2}, n=\frac{t}{2}} = \frac{3 s^2 t^2}{(s+t)^3}, \quad (4.8)$$

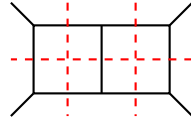
where the factor of proportionality is fixed by the β integral in Eq. (4.4). At one loop the $c_{mn}^{(2)}$ are obtained studying $\log^2 U \log^2 V$ term in the correlation function, so what we get seems in accordance with the identification of the double spectral density ρ_{st} and CFT qDisc [56], which selects exactly this term. The qDisc of a correlator is defined as the quadruple discontinuity obtained by taking one double discontinuity in $\bar{z} = 1$, followed by a dDisc around $z = 0$, in this way one focuses on terms which have at least a $\log^2(1 - \bar{z})$ and a $\log^2 z$. Performing a

¹³Amplitudes of spinless massive particles under certain specific assumptions can be expressed through the following representation:

$$\mathcal{A}(s, t) = \text{poles} + \frac{1}{\pi^2} \iint \frac{\rho_{st}(s', t')}{(s' - s)(t' - t)} ds' dt' + \frac{1}{\pi^2} \iint \frac{\rho_{tu}(t', u')}{(t' - t)(u' - u)} dt' du' + \frac{1}{\pi^2} \iint \frac{\rho_{su}(s', u')}{(s' - s)(u' - u)} ds' du'$$

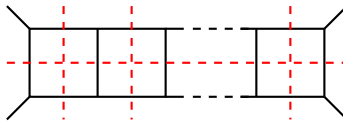
where $\rho_{xy} = \text{disc}_x \text{disc}_y \mathcal{A}$ is called the double spectral density.

similar analysis at two loops, we find¹⁴



$$\propto c_{mn} \Big|_{m=\frac{s}{2}, n=\frac{t}{2}} = -\frac{3t^5}{256} {}_2F_1 \left(D-4, D-4, \frac{3}{2}(D-4); -\frac{t}{s} \right) \Big|_{D=10}. \quad (4.9)$$

We conjecture that the same should happen at higher loops, i.e. that in flat space the $c_{mn}^{(\kappa)}$'s in Eq. (4.5) reproduce the *maximal cut* of the corresponding κ rungs ladder diagrams, where the *maximal cut* corresponds to the diagram with all the propagators on-shell. Following similar ideas as in Sec. 3.2 we can construct the maximal cut contribution for the ladder diagram as an iterated integral. In order to do so we apply the loop-by-loop construction of the Baikov representation [57] obtaining¹⁵



$$c_{mn}^{(\kappa)} \Big|_{m=\frac{s}{2}, n=\frac{t}{2}} \sim \int_0^{t/s} dZ c_{mn}^{(\kappa-1)}(s, t) \Big|_{t=sZ} \frac{F_b^5(s, t, Z)}{G^3(s, t)}, \quad (4.10)$$

where we have defined the Gram determinant and the cut Baikov kernel as:

$$G = \frac{1}{4} st(s+t) \quad F_b = \frac{1}{4} s(t-sZ). \quad (4.11)$$

We have also tested that the contribution of this maximal cut, after having performed the integration associated with the discontinuity in t , matches up to polynomial terms the one obtained with (3.23).

Acknowledgements

We thank F. Alday and E. Perlmutter for several discussions and insights. AG also thanks B. Page, S. Abreu, B. Basso, E. Trevisani, V. Goncalves, R. Pereira, G. Korchemsky for useful discussion. The work of AB and GF is supported by Knut and Alice Wallenberg Foundation under grant KAW 2016.0129 and by VR grant 2018-04438. The work of AG is supported by the Knut and Alice Wallenberg Foundation under grant 2015.0083 and by the French National Agency for Research grant ANR-17-CE31-0001-02 and ANR-17-CE31-0001-01.

¹⁴At a first glance, this should be surprising, since it is involved a “triple-trace” type of cut, however a more careful analysis shows that c_2 in Eq. (3.10) does not really contribute.

¹⁵The analysis is dimensional independent but here we present the explicit results in ten dimensions.

A Harmonic Polylogarithms

Harmonic Polylogarithms [58–60] are a generalization of the classical polylogarithms and similarly can be defined through some iterated integrations. We will denote with $H_{\dots}(x)$ the harmonic polylogarithm of argument x and transcendental weight w , where the dots represent a collection of w indices. Starting from weight one,

$$H_0(x) = \log(x) \quad H_1(x) = -\log(1-x) \quad H_{-1}(x) = \log(1+x), \quad (\text{A.1})$$

we can generate all the HPL's of higher transcendentality as

$$H_{a\dots}(x) = \int_0^x dx' H_{\dots}(x') \phi(a, x') \quad (\text{A.2})$$

with

$$\phi(0, x) = \frac{1}{x} \quad \phi(1, x) = \frac{1}{1-x} \quad \phi(-1, x) = \frac{1}{1+x}. \quad (\text{A.3})$$

From this definition it is clear that the usual polylogarithms takes the form $\text{Li}_n(x) = H_{\vec{0}_{n-1}}(x)$. These new functions present lots of interesting properties and advantages, one among others is that it is easy to study their analytic behaviour. In particular, HPL's with only 0's and 1's in their index vector, can develop only two types of logarithmic singularity, one at $x = 0$ and the other one at $x = 1$, that can be directly detected looking at the index vector itself. Divergences of type $\log^n x$ arises when there are n 0's to the right end of the weight vector, while if n 1's appear to the very left, the HPL will behave as $\log^n(1-x)$ for $x \rightarrow 1$. The ease of extracting singular behaviour will be really useful when comparing CFT computations and amplitude results.

B The two loop example

In this Appendix we will report in more detail the results in [10] for the two-loop example. We will first give the full answer for the highest logarithmic term of the correlation function of four identical \mathcal{O}_2 operators at order c^{-3} , then we will continue with a discussion of the two-loop amplitude, giving full results for the planar and non planar double box integrals. We continue with some comments on the comparison between these two results. In the last section, we perform a parallel two-loop analysis in Mellin space. We refer to the ancillary Mathematica file for the longer expressions.

B.1 Results for $\mathcal{H}^{(3)}|_{\log^3(z\bar{z})}$

Let us start from the the expression for $h^{(3)}(z)$, according to Eq. (2.45) and (2.49), it takes the form

$$h^{(3)}(z) = p_3 \left(\frac{z}{z-1} \right) (H_{001}(z) + H_{101}(z)) + p_3(z) (H_{001}(z) + H_{011}(z)) \quad (\text{B.1})$$

$$+ q_3(z)H_{01}(z) + q_3 \left(\frac{z}{z-1} \right) (H_{01}(z) + H_{11}(z)) + j_1(z)H_1(z) + j_0(z)$$

$$p_3(z) = -\frac{(10z^2 + 10z + 1)}{2880z^5} \quad (\text{B.2})$$

$$q_3(z) = \frac{1260z^4 - 3870z^3 + 4170z^2 - 1785z + 227}{172800z^5} \quad (\text{B.3})$$

$$j_1(z) = \frac{(1258z^3 - 4161z^2 + 5806z - 2903)}{172800z^4} \quad (\text{B.4})$$

$$j_0(z) = -\frac{217855z^3 - 685424z^2 + 749142z - 499428}{12441600z^3} \quad (\text{B.5})$$

Now applying Eq. (2.31), we can extract¹⁶

$$\begin{aligned} \mathcal{H}^{(3)}(z, \bar{z}) \Big|_{\log^3(z\bar{z})} &= \frac{(z\bar{z})^2}{25(z-\bar{z})^{23}} \{ R_1(z, \bar{z})H_{001}(z) + R_2(z, \bar{z})H_{011}(z) + R_3(z, \bar{z})H_{101}(z) \\ &+ R_4(z, \bar{z})H_{01}(z) + R_5(z, \bar{z})H_{11}(z) + \left(R_6(z, \bar{z}) - \frac{\pi^2(2R_3(z, \bar{z}) - R_2(z, \bar{z}))}{6} \right) H_1(z) \\ &- (z \leftrightarrow \bar{z}) + R_7(z, \bar{z}) \} , \end{aligned} \quad (\text{B.6})$$

where R_i are polynomials of degree 30 in z, \bar{z} such that $R_i(z, \bar{z}) = R_i(\bar{z}, z)$ for $i = 1, 2, 3, 7$. We compute the flat space limit following the procedure explained in Sec. 2.3:

$$\frac{\text{dDisc}[z\bar{z}(\bar{z}-z)]\mathcal{H}^{(3)}(z^\circ, \bar{z})|_{\log^3(z\bar{z})}}{4\pi^2} \xrightarrow{\text{flat space}} 2\pi i \frac{\Gamma(22)}{(2x)^{22}} \log(1-\bar{z})g^{(3)}(\bar{z}), \quad (\text{B.7})$$

$$\begin{aligned} g^{(3)}(\bar{z}) &= \frac{(\bar{z}-1)^6}{3456000\bar{z}^8} \{ -60(21\bar{z}^5 - 30\bar{z}^4 + 10\bar{z}^3 - 10\bar{z}^2 + 30\bar{z} - 21)H_{11}(\bar{z}) \\ &+ 60(10\bar{z}^2 - 30\bar{z} + 21)H_{10}(\bar{z}) - 60(21\bar{z}^2 - 30\bar{z} + 10)\bar{z}^3H_{01}(\bar{z}) \\ &+ (-2\bar{z}^5 + 1245\bar{z}^4 - 1290\bar{z}^3 + 1290\bar{z}^2 - 60i\pi(10\bar{z}^2 - 30\bar{z} + 21) - 1245\bar{z} + 2)H_1(\bar{z}) \\ &- (2\bar{z}^4 + 15\bar{z}^3 + 120\bar{z}^2 - 1170\bar{z} + 1260)\bar{z}H_0(\bar{z}) - 10\pi^2(21\bar{z}^2 - 30\bar{z} + 10)\bar{z}^3 \\ &+ (-1258\bar{z}^3 + 871\bar{z}^2 - 871\bar{z} + 1258)\bar{z} + i\pi(2\bar{z}^4 + 15\bar{z}^3 + 120\bar{z}^2 - 1170\bar{z} + 1260)\bar{z} \} . \end{aligned} \quad (\text{B.8})$$

¹⁶To adapt to our convention we have restored the factor $(z\bar{z})^2$ and we have multiplied everything by $4^3 \cdot 2 \cdot 3$

Remember that what we have found is only part of the dDisc, in fact at $\kappa = 3$ also $\log^2(z\bar{z})$ contributes, and since unfortunately we have not access to this information, we can not fully reconstruct the correlator. Given the incompleteness of our answer, we expect that we can not perfectly compare our result with the amplitude computed on the gravity side. We have further discussed these issues in Sec. 3.1.

B.2 Two loop SUGRA Amplitude

The ten dimensional flat space graviton amplitude at two loops has been studied in [61, 62], however these works concentrate only on divergent parts, while for our purposes we need to know the full answer, finite part included. To obtain it, we have to compute the two-loop diagrams (see Fig. 2) appearing in Eq. (3.1) and to do so we will use the method of differential equations [63–73]. Let us briefly describe how the method works as it will also be useful to understand how the discontinuity and the cuts are constructed. The differential equations are constructed by differentiating the integral of interest with respect to the kinematic invariants, in our case the only dependence is on the ratio t/s . The integrals appearing after the differentiation are not the starting ones, but can be reduced to a set of Master Integrals (MI) by integral by parts identities (IBP) [74]. So in general one wants to apply the differentiation on the MI's as all the others can be expressed as a linear combinations of them. In the case of interest the integrals contributing are depicted below in Eq. (B.9), where the dashed line represents a numerator constructed from the associated loop momenta and the opposite external momenta. The next step in order to solve the system of differential equations is to construct a canonical basis: different results and algorithms to obtain it can be found in [70, 75–78] for the diagrams we are considering. We report our choice for the planar diagram¹⁷, the one we will be focusing on

$$\begin{aligned}
I_1 &= -2\epsilon(2\epsilon - 1)(3\epsilon - 2)(3\epsilon - 1) \text{ (Diagram 1)} & I_2 &= -\frac{s}{t}2\epsilon(2\epsilon - 1)(3\epsilon - 2)(3\epsilon - 1) \text{ (Diagram 2)} \\
I_3 &= \frac{1}{2}\epsilon^2(2\epsilon - 1)(3\epsilon - 1) \text{ (Diagram 3)} & I_4 &= \epsilon^2(2\epsilon - 1)^2 \text{ (Diagram 4)} \\
I_5 &= 3I_3 + 3\epsilon^3(2\epsilon - 1) \text{ (Diagram 5)} & I_6 &= -\frac{\epsilon^4(s+t)}{s} \text{ (Diagram 6)} \\
I_7 &= -\frac{t}{s}\epsilon^4 \text{ (Diagram 7)} & I_8 &= \epsilon^4 \text{ (Diagram 8)}
\end{aligned} \tag{B.9}$$

The coefficients are chosen to make them uniform transcendental in $d = 4 - 2\epsilon$ dimensions [68]. From the solution of these differential equation system we were able to find the expressions

¹⁷A basis for the non planar one can be found here [79].

for the planar and similarly for the non planar double box diagrams. For simplicity, we have chosen the basis integrals and solved the equations in four dimensions. Once the results are known in 4d, it is indeed possible to uplift them to ten dimensions by means of dimensional recurrence relations¹⁸ [80–82].

We now present the full results for the planar and non planar integrals in Fig. 2¹⁹.

$$I_{db}^{pl}(s, t) = \int \frac{d^{10}l_1}{(2\pi)^{10}} \frac{d^{10}l_2}{(2\pi)^{10}} \frac{1}{l_1^2(p_1 + l_1)^2(p_1 + p_2 + l_1)^2(l_1 + l_2)^2l_2^2(p_4 + l_2)^2(p_3 + p_4 + l_2)^2} \quad (\text{B.10})$$

$$= \frac{(-s)^{3-2\epsilon}}{(4\pi)^{10}} \left\{ -\frac{2}{7!5!} \frac{4s+t}{s\epsilon^2} - \frac{22384s^3 + 6247s^2t + 252st^2 + 63t^3}{70 \cdot 10!s^3\epsilon} + \frac{8s^6}{5t^3(s+t)^3} I_{(0)}^{pl}(s, t) \right\}. \quad (\text{B.11})$$

The finite part, which is the one relevant for us, is:

$$I_{(0)}^{pl}(s, t) = -p_3 \left(\frac{s}{s+t} \right) H_{-1-100} + q_3 \left(-\frac{s}{t} \right) H_{-100} + P_1(s, t)H_{00} + P_2(s, t)H_0 + P_3(s, t) \\ + \frac{1}{6}p_3 \left(\frac{s}{s+t} \right) \left(\pi^2 (H_{-10} - 3H_{-1-1}) - 6\zeta_3 H_{-1} \right) + q_3 \left(-\frac{s}{t} \right) \left(\frac{1}{6}\pi^2 (3H_{-1} - H_0) + \zeta_3 \right), \quad (\text{B.12})$$

where $H_{\dots} \equiv H_{\dots} \left(\frac{t}{s} \right)$, p_3 and q_3 are the functions introduced in Eqs. (2.50) and (2.51). The P_i 's are given by

$$P_1(s, t) = \frac{2t^2 (8820s^7 + 40320s^6t + 72765s^5t^2 + 64575s^4t^3 + 28098s^3t^4 + 4872s^2t^5 + 90st^6 + 10t^7)}{8!5!s^7(s+t)^2} \quad (\text{B.13})$$

$$P_2(s, t) = -\frac{t^2 (52920s^8 + 206640s^7t + 303975s^6t^2 + 202440s^5t^3 + 55111s^4t^4 + 2912s^3t^5 - 29s^2t^6 - 72st^7 - 9t^8)}{108!s^9(s+t)}$$

$$P_3(s, t) = -\frac{t}{15680 \cdot 10!s^9(s+t)^2} \left[t(s+t)^2 (-51861600s^7 - 149838032s^6t - 135584013s^5t^2 - 24845515s^4t^3 \right. \\ \left. + 17602466s^3t^4 + 5332598s^2t^5 + 622251st^6 + 83013t^7) + 3920\pi^2s^2 (17640s^8 + 67410s^7t + 84034s^6t^2 \right. \\ \left. + 15834s^5t^3 - 47172s^4t^4 - 37074s^3t^5 - 8544s^2t^6 - 225st^7 - 25t^8) \right] \quad (\text{B.14})$$

For the non planar contribution we obtain

$$I_{db}^{np}(s, t) = \int \frac{d^{10}l_1}{(2\pi)^{10}} \frac{d^{10}l_2}{(2\pi)^{10}} \frac{1}{l_1^2(p_1 + l_1)^2(p_1 + p_2 + l_1)^2(l_1 + l_2)^2l_2^2(p_4 + l_2)^2(p_3 - l_1 - l_2)^2} \quad (\text{B.15})$$

$$= \frac{(-s)^{3-2\epsilon}}{(4\pi)^{10}} \left\{ \frac{1}{5!6!\epsilon^2} + \frac{917s^2 + 2t(-s-t)}{3 \cdot 10!s^2\epsilon} + \frac{1}{25 \cdot 9!s^4(s+t)^3} I_{(0)}^{np}(s, t) \right\}. \quad (\text{B.16})$$

¹⁸By similar reasoning one can prove that the differential equations in Fuchsian form is actually $d \pm 2$ invariant.

¹⁹As we will see, the $\mathcal{O}(\epsilon^{-1})$ does not match exactly the one in [61] because we have not explicitly subtracted the one loop pole.

The finite part takes the form

$$\begin{aligned}
I_{(0)}^{np}(s, t) &= S_1(s, t) (H_{-3} + H_{-20} - 2H_{-100}) + \frac{(s+t)^3 S_1(s, u)}{t^3} (2H_{-2-1} - H_{-1-2} - H_{-1-10}) \\
&+ H_{-10} \left(\frac{1}{60} S_2(s, t) + \frac{i\pi(s+t)^3 S_1(s, u)}{t^3} \right) + H_{-2} \left(\frac{1}{60} S_2(s, t) - \frac{2i\pi(s+t)^3 S_1(s, u)}{t^3} \right) \\
&+ H_{00} \left(-\frac{(s+t)^3 S_3(s, u)}{60t^3} - i\pi S_1(s, t) \right) + \frac{1}{60} S_3(s, t) H_{-1-1} \\
&+ H_{-1} \left(\pi^2 \left(-\frac{(s+t)^3 S_1(s, u)}{2t^3} - S_1(s, t) \right) - \frac{1}{60} i\pi S_3(s, t) + \frac{1}{360} S_4(s, t) \right) \\
&+ H_0 \left(-\frac{(s+t)^3 S_4(s, u)}{360t^3} + \frac{1}{2} \pi^2 S_1(s, t) - \frac{1}{60} i\pi S_2(s, t) \right) \\
&+ \frac{1}{120} \pi^2 \left(-\frac{(s+t)^3 S_3(s, u)}{t^3} + S_2(s, t) + 2100s^4(s+t)^3 \right) + \zeta(3) S_5(s, t) \\
&- \frac{1}{2} i\pi^3 S_1(s, t) - \frac{1}{360} i\pi S_4(s, t) + \frac{S_6(s, t)}{7560}, \tag{B.17}
\end{aligned}$$

where again we have defined the polynomials appearing as:

$$\begin{aligned}
S_1(s, t) &= t^5 (15s^2 + 10st + 2t^2) \\
S_2(s, t) &= \frac{(s+t)}{s^4 t^2} (-420s^{12} - 2370s^{11}t - 5270s^{10}t^2 - 5525s^9t^3 - 2209s^8t^4 + 389s^7t^5 + 171s^6t^6 \\
&+ 1664s^5t^7 + 3866s^4t^8 + 4500s^3t^9 + 3100s^2t^{10} + 1200st^{11} + 200t^{12}) \\
S_3(s, t) &= \frac{(s+t)^8 (720s^8 - 1280s^7t + 249s^6t^2 + 78s^5t^3 - 366s^4t^4 + 400s^3t^5 - 300s^2t^6 + 200st^7 - 200t^8)}{s^4 t^5} \\
S_4(s, t) &= \frac{(s+t)^2}{s^3 t^4} (-4320s^{12} - 16080s^{11}t - 4974s^{10}t^2 + 61465s^9t^3 + 120276s^8t^4 + 88029s^7t^5 \\
&+ 15996s^6t^6 - 7880s^5t^7 + 1296s^4t^8 + 9800s^3t^9 + 10000s^2t^{10} + 5400st^{11} + 1200t^{12}) \\
S_5(s, t) &= 3 (40s^7 + 110s^6t + 84s^5t^2 + 15s^2t^5 + 10st^6 + 2t^7) \\
S_6(s, t) &= \frac{1}{s^2 t^3} (45360s^{12} + 236880s^{11}t + 280917s^{10}t^2 + 24169796s^9t^3 + 72161380s^8t^4 + 71728624s^7t^5 \\
&+ 23275934s^6t^6 - 639392s^5t^7 - 369323s^4t^8 - 278250s^3t^9 - 194250s^2t^{10} - 75600st^{11} - 12600t^{12})
\end{aligned}$$

Let us briefly comment on the amplitude divergences: as we can see from Eq. (B.11) and (B.16), at two loops the combination $(I_{db}^{pl}(s, t) + I_{db}^{np}(s, t) + t \leftrightarrow u)$, appearing in the amplitude, cancels the divergence at order ϵ^{-2} , thus making the discontinuity convergent. At higher loops, instead, we do expect a divergence of order $1/\epsilon^2$ and consequently a divergent discontinuity of \mathcal{A}_{10}^{sugra} . So in principle for $\kappa > 3$, if we wanted to compare dDisc with the discontinuity of the amplitude, it would be necessary to renormalize the latter subtracting

the lower loops poles. At the same time, it exists an object derived from the amplitude, which is always finite in ten dimensions, the iterated s -channel cut mentioned before, this can be naturally compared to the CFT without the need of any renormalization procedure.

B.3 Match Amplitude and CFT at 2 loops

Here we report the results for the discontinuity of \mathcal{A}_{10}^{sugra} at two loops and its comparison with the flat space limit of $d\text{Disc}\mathcal{H}^{(3)}|_{\log^3(z\bar{z})}$ as described in Sec. 3.1.

The first important remark is that the quantity computed from the CFT correlator should not be compared with the discontinuity of the entire amplitude, but rather with only one channel and restricting to the planar contribution. In particular, in our convention, we have to consider $\text{disc}_{x>1} F_{3,pl}^t(x)$, where $F_{3,pl}^t(x)$ contains the contributions from $t^2(I_{db}^{pl}(t, s) + s \leftrightarrow u)$. Before performing the discontinuity, we have defined the amplitude in the correct physical region through the appropriate analytic continuations. Finally to connect with the CFT results, we have expressed everything as a function of \bar{z} , through the identification $\bar{z} = \frac{1}{x}$. We collect the results of this comparison in the table below, where we have defined $\mathcal{Q}_{CFT} \equiv \frac{i\pi(\bar{z}-1)^{11}}{10\bar{z}^8} \log(1 - \bar{z})g^{(3)}(\bar{z})$ and $\mathcal{Q}_{Ampl} \equiv \frac{i\pi(\bar{z}-1)^{11}}{10\bar{z}^8} \text{disc}F_{3,pl}^t(\bar{z})$.

	H_{111}	H_{110}	H_{011}	H_{101}	H_{001}	H_{11}	H_{10}	H_{01}	H_1	H_0
\mathcal{Q}_{CFT}	$-3(\tilde{p}_3 + p_3)$	$-2p_3$	$-2\tilde{p}_3$	$-\tilde{p}_3 - p_3$	0	$2(\tilde{q}_3 + q_3 + i\pi p_3)$	\tilde{q}_3	\tilde{q}_3	$-j_1 - i\pi\tilde{q}_3 - \frac{\pi^2}{6}\tilde{p}_3$	0
\mathcal{Q}_{Ampl}	$-\tilde{p}_3 - p_3$	$-p_3$	$-\tilde{p}_3$	$-\tilde{p}_3$	$-\tilde{p}_3$	$\tilde{q}_3 + q_3 + i\pi p_3$	\tilde{q}_3	q_3	$\tilde{P}_1 + P_1 - i\pi\tilde{q}_3 + \frac{\pi^2 p_3}{6}$	\tilde{P}_1

Here $H_{\dots} \equiv H_{\dots}(\bar{z})$ is the Harmonic polylogarithm, p and q are the polynomials in Eqs. (2.50) and (2.51), while j_1 and P_1 are respectively introduced in Eq. (B.4) and (B.14). For convenience we have defined $p_3(1 - \bar{z}) \equiv p_3$ and $p_3\left(\frac{\bar{z}-1}{\bar{z}}\right) \equiv \tilde{p}_3$ and analogously for all the other polynomials.

As already said, we notice that the two contributions do not match exactly: some terms do not appear or appear with different coefficients on the two sides. Interestingly if one extracts the logarithmic singularities from the HPL's, as explained in Appendix A, and ignoring weight one and zero terms, all the functions multiplying $\log^n(1 - \bar{z})$ in the CFT actually coincide with the ones appearing in the amplitude, but with a factor n of difference (as can be already deduced from the table above). This fact is another indication of why c_{dc} reproduces $g^{(3)}(\bar{z})$ upon the log-factorization. In particular the factor of three of difference in the leading $\log(1 - \bar{z})$ term is exactly the one necessary to have their perfect agreement.

The contributions to the discontinuity coming from the other channels in \mathcal{A}_{10}^{sugra} at order c^{-3} can be partially recovered considering crossing symmetric versions [83] of $\mathcal{H}^{(3)}|_{\log^3(z\bar{z})}$, to be precise

$$\mathcal{H}^{(3)}(u, v) = \frac{u^2}{v^2} \mathcal{H}^{(3)}(v, u) \leftrightarrow s \text{ channel}, \quad (\text{B.18})$$

$$\mathcal{H}^{(3)}(u, v) = \frac{u^2}{v^2} \mathcal{H}^{(3)}\left(\frac{1}{v}, \frac{u}{v}\right) \leftrightarrow u \text{ channel}. \quad (\text{B.19})$$

Also in these two other channels the match is not perfect and we encounter the same type of discrepancies found before.

We can now pass to analyse the c_1 and c_2 type of discontinuities, they can be computed exploiting the same differential equation method introduced before. Cut diagrams do indeed satisfy the same system of equations [57, 84] but now with different boundary conditions and where only a sub-set of topologies contribute. To be more precise, the diagrams contributing to each cut will be the ones where the onshell propagators are present and in the case at hand we find

$$\begin{aligned}
c_1 : & \quad \text{[Diagram with vertical red dashed line]} \rightarrow \text{[Diagram with vertical black line]} + \text{[Diagram with horizontal black line]} + \text{[Diagram with two circles]} + \text{[Diagram with a triangle]}, \\
c_2 : & \quad \text{[Diagram with diagonal red dashed line]} \rightarrow \text{[Diagram with vertical black line]} + \text{[Diagram with diagonal black line]} + \text{[Diagram with a circle]}.
\end{aligned}$$

Each solution is fixed up to a boundary condition that unfortunately we were not able to fix separately, we could express one condition in term of the other by requiring that

$$\text{disc}_s I_{db} = 2\pi i \left(\mathcal{A}|_{c_1} + \mathcal{A}|_{c_2} \right). \quad (\text{B.20})$$

However, since in the CFT we expect that higher $\log(1 - \bar{z})$ powers are fixed by double trace contributions, we can use this insight to partially fix these boundary conditions. We can compare again $\text{dDisc}\mathcal{H}^{(3)}|_{\log^3(z\bar{z})}$ with $\text{disc}\mathcal{A}_{10}^{\text{supra}}$, but now we can distinguish and analyse separately c_1 and c_2 . The table below contains the result of this comparison, we report the weight three and two functions appearing in Eq. (B.7) and in c_1 and c_2 respectively with the corresponding polynomial coefficients properly normalized.

	H_{111}	H_{110}	H_{011}	H_{101}	H_{001}	H_{100}	H_{11}	H_{10}	H_{01}	H_{00}
CFT	$-3(p_3 + \tilde{p}_3)$	$-2p_3$	$-2\tilde{p}_3$	$-(p_3 + \tilde{p}_3)$			$2(q_3 + \tilde{q}_3)$	\tilde{q}_3	\tilde{q}_3	
c_1	$-(p_3 + \tilde{p}_3)$	$-p_3$	$-\tilde{p}_3$	$-p_3$		$-p_3$	$q_3 + \tilde{q}_3$	\tilde{q}_3	\tilde{q}_3	\tilde{q}_3
c_2				$p_3 - \tilde{p}_3$	$-\tilde{p}_3$	p_3			$q_3 - \tilde{q}_3$	$-\tilde{q}_3$

where again all H are $H_{...}(\bar{z})$.

The two cuts present lots of similarities in the polynomial structure but a different singular behaviour. The similarities of the polynomial structure are expected as they come from the same starting integral and it partially explains why, when they mix in the full discontinuity, give rise to something which resembles the CFT computation but with all the discrepancies we observe. Even after having separated the two contributions, c_1 still does not reproduce the first row of this table, we believe that these differences derive from part of the $\log^2 U$ term in the correlator.

The last object we have introduced in Sec. 3.1 is the *double cut*. Analogously to what we have done before, this can be constructed from the differential equations where now only one subtopology contributes,

$$c_{dc} : \quad \text{[Diagram with two vertical red dashed lines]} \rightarrow \text{[Diagram with vertical black line]} + \text{[Diagram with two circles]}. \quad (\text{B.21})$$

With a suitable choice of boundary conditions we can fix c_{dc} in such a way that it matches Eq. (B.7) up to a $\log(1 - \bar{z})$ factorization as in Eq. (3.11). Let us comment on the advantages of computing this iterated cut directly from the differential equations: it is computationally easier because we can reuse the results from the previous computations and most importantly in this way we avoid the need to specify any $i\epsilon$ prescription, that are in general not well defined in the case of multiple discontinuities.

To conclude, let us spend a few words on the possible contributions of the non planar double box diagram. As can be derived from Eq. (B.17), the integral can contain only terms of transcendental weight two or lower, to be precise the subset of HPLs appearing in the t -channel is made by $\{H_{01}, H_{10}, H_{00}, H_1, H_0\}$. The reasons why we have decided not to include it in the previous discussion are one practical and one more conceptual. The first one comes from the direct computation of the discontinuity that gives polynomials with a structure completely different from the ones we have been considering. The second one relies on the fact that we believe that the discontinuity associated to the non planar box should be reproduced by part of the $\log^2 U$ piece of $\mathcal{H}^{(3)}$ that unfortunately we are not able to compute. To do so it would be indeed necessary to completely solve the mixing problem up to order c^{-2} and to find a way to include triple trace operators and unfortunately neither of these problems have been tackled yet.

B.4 Two-loop Mellin amplitude

As anticipated in Sec. 4.1, for the Mellin amplitude associated to $\mathcal{H}^{(3)}|_{\log^3(z\bar{z})}$, which we remind behaves like as $\sim \log^3 U \log^2 V$ in the double expansion around small U and V , one can consider the following ansatz:

$$\widetilde{\mathcal{M}}_{\log}^{(3)}(s, t) = \sum_{m, n=2} \frac{c_{mn}}{(s - 2m)^2(t - 2n)} + \text{cyclic permutation} . \quad (\text{B.22})$$

Plugging this expression, without considering the permutations, in Eq. (4.1) and comparing the resulting $\log^3 U \log^2 V$ terms with the corresponding ones in the correlator of Eq. (B.6), one can fix the $c_{mn}^{(3)}$:

$$c_{mn}^{(3)} = \frac{r^{(12)}(m, n)H_{m+n-1}}{(n-1)_7} + \sum_{i=0}^6 \left(\frac{r_{1,i}^{(8)}(m)H_{m-i}}{n+i-1} + \frac{r_{2,i}^{(8)}(m)}{m+n-1-i} \right) . \quad (\text{B.23})$$

The $r^{(j)}$ are polynomials of degree j in the corresponding variables, see the ancillary Mathematica file for their explicit expressions.

Now the flat space limit can be taken allowing s, t to go to infinity, however, given the form of Eq. (B.22), this is not obvious and needs to be taken carefully. Retracing the same steps of [15], let us start by focusing on one channel of our Mellin amplitude and consider

$$\widetilde{\mathcal{M}}_{\log, 1ch}^{(3)} = \sum_{m, n=2}^{\infty} \frac{c_{mn}^{(3)}}{(s - 2m)^2(t - 2n)} . \quad (\text{B.24})$$

First of all notice that this series is divergent. To regularize it, we take as many derivatives in s and t as the ones necessary to make it convergent²⁰. Then, the flat space limit is implemented by taking $s, t \rightarrow \infty$ with m and n of the same order. In this regime, the sums can be replaced by integrals and eventually we are left with

$$\partial_s^2 \partial_t^3 \widetilde{\mathcal{M}}_{\log, 1ch}^{(3)} \simeq \int_0^\infty dm dn \frac{-10! m^{11}}{20n^3(m+n)^3} \frac{-p_3(m/m+n) \log\left(1 + \frac{n}{m}\right) + q_3(-m/n)}{(s-2m)^4(t-2n)^4}, \quad (\text{B.25})$$

where the polynomials p_3 and q_3 are defined in Eq. (B.2) and (B.3)²¹. Notice the similarity with the amplitude (the same permutations are involved) and in particular with the form of the planar double box integral in Eq. (B.12).

In analogy with the one-loop example, one would expect that, when integrated in m and n , Eq. (B.25) gives derivatives of the two-loop amplitude in the corresponding channel²² or at least part of it. However this seems not to be the case.

Let us start considering the integral of Eq. (B.25), this reads

$$\partial_s^2 \partial_t^3 \widetilde{\mathcal{M}}_{\log, 1ch}^{(3)} = \frac{1}{s} \left(f_1(t/s) \left(H_{-100} + \frac{\pi^2}{2} H_{-1} \right) + f_2(t/s) \left(H_{00} + \frac{\pi^2}{2} \right) + f_3(t/s) H_0 + f_4(t/s) \right) \quad (\text{B.26})$$

with $H_{\dots} \equiv H_{\dots} \left(\frac{t}{s} \right)$. If we compare the previous expression with the derivatives of the amplitude, we observe that:

- i) The maximum degree of transcendentality of the functions in Eq. (B.26) is one degree less than the one in the amplitude, where even after taking derivatives, they appear HPL's of weight four and lower.
- ii) If one imagines to integrate back the derivatives in s and t , then $\widetilde{\mathcal{M}}_{\log, 1ch}^{(3)} \sim s^4$, which does not match again the amplitude ($\sim s^5$). Moreover, this behaviour seems to be in contrast with the general prescription in [86]: here the authors find a relation between the way in which the correlator diverges in the bulk point limit and the polynomial growth of the Mellin amplitude. According to their prediction a singularity $\sim (z - \bar{z})^{-23}$, which is the one we are considering, should produce a Mellin amplitude that goes²³ as s^5 , in accordance with the flat space amplitude result we have.
- iii) If one ignores what said before and nonetheless tries to enforce a comparison with the amplitude, one soon realizes that, in order to at least reproduce the structure of the polynomials f_i , it is necessary to take one s derivative more of the amplitude, i.e. to

²⁰We have verified that keeping the total number of derivatives fixed, reshuffling between s and t derivatives determines only the appearance of a factor of $\frac{s}{t}$ to some power and a change in the polynomial term.

²¹The same result was recently obtained in [85] in a completely different set-up.

²²In this context, we has to consider the amplitude as in Eq. (3.1) without the \hat{K} factor, as we have already accounted for it in Θ_4^{flat} . Moreover, notice that this number of derivatives kills the divergent parts.

²³If one applies formula (217) of [86] with $\Delta = 2$, one find s^9 , however we need to remember that in $\widetilde{\mathcal{M}}$ we have stripped out a factor s^4 , so the two results are consistent.

consider $\partial_s^3 \partial_t^3 \left(s^2 I_{db}^{pl}(s, t) \right)$. This indeed gives

$$\begin{aligned} \partial_s^3 \partial_t^3 \left(s^2 I_{db}^{pl}(s, t) \right) &= \frac{16}{14175 s} \left(f_1(t/s) \left(H_{-1-100} - \frac{\pi^2}{6} H_{-10} + \frac{\pi^2}{2} H_{-1-1} + \zeta_3 H_{-1} \right) \right. \\ &+ f_2(t/s) \left(H_{-100} + \frac{\pi^2}{2} H_{-1} - \frac{\pi^2}{6} H_0 + \zeta_3 \right) + (\tilde{f}_3(t/s) - \tilde{f}_3(t/s)) H_{00} + \tilde{f}_4(t/s) H_0 \\ &\left. - \tilde{f}_4(t/s) H_0 + f_5(t/s) \pi^2 + f_6(t/s) \right). \end{aligned} \quad (\text{B.27})$$

These observations motivated the study of the maximal cut in Eq. (4.9). Then reinterpreting the problem from this perspective and in light of our discussion in Sec. 4.1, we should have somehow expected not to reproduce the full amplitude starting from (B.25), in fact there is not a dispersion relation representation constructed from such multiple discontinuities. Moreover, given the fact that we are taking only a double integral, it seems more reasonable why we should take an additional derivative and why we do not get functions with the right transcendentality. For all these reasons we have decided to try to compare Eq. (B.26) with our results for c_1 and c_2 , looking for some similarities and connections. So let us consider

$$\begin{aligned} \partial_s \left(\partial_s^2 \partial_t^3 \left(\text{Diagram 1} \right) \right)_{\pi^0 \text{ terms}} &= \frac{16}{14175 s} \left(f_1(t/s) H_{-100} + f_2(t/s) H_{00} + \tilde{f}_3(t/s) H_0 + \tilde{f}_4(t/s) \right), \\ \partial_s \left(\partial_s^2 \partial_t^3 \left(\text{Diagram 2} \right) \right)_{\pi^0 \text{ terms}} &= \frac{-16}{14175 s} \left(f_1(t/s) (H_{-100} - H_{-1-10}) + f_2(t/s) (H_{00} - H_{-10}) \right. \\ &\left. + \tilde{f}_3(t/s) H_0 + \tilde{f}_4(t/s) \right). \end{aligned}$$

Comparing them with Eq. (B.26), we notice that the highest transcendentality pieces here are correctly reproduced by c_1 . The results for c_2 are very similar, but this is inevitable since they come from the same terms in the amplitude. The relevant fact is instead that if we sum up the two contributions the characteristic structure of Eq. (B.26) is completely lost, thus signalling again the need to distinguish the two types of cuts. The qualitative idea motivating the comparison of the Mellin result and the additional derivative of the discontinuities is that starting from a double pole in s and a simple one in t , performing a double integral is not sufficient and we are left with a s pole still to be solved. However these are, as said, qualitative observations based on the example at hand and we were not able to get to a better and more rigorous explanation.

Let us conclude by a brief comment on the lower $\log U$, $\log V$ -powers coming from the residue integral defining the Mellin transform, once we plug in the expression for $\widetilde{\mathcal{M}}_{\log, 1ch}^{(3)}$.

As anticipated in Sec. 4.1,

$$\begin{aligned} \mathcal{H}^{(3)}(U, V) = & \sum_{m,n=2}^{\infty} \frac{(n-1)_{m+1}^2 c_{mn}}{24\Gamma(m-1)^2} U^m V^{n-2} \log^3 U \log^2 V + \\ & \frac{(n-1)_{m+1}^2 c_{mn}}{4\Gamma(m-1)^2} U^m V^{n-2} (H_{m+n-1} - H_{m-2}) \log^2 U \log^2 V + \dots \end{aligned} \quad (\text{B.28})$$

The second term is the one we expect to derive from simple poles in s and t , so we argue that the unknown parts of $\mathcal{H}^{(3)}$ should have a Mellin representation including

$$\sum_{m,n} \frac{6c_{mn}^{(3)}(H_{m+n-1} - H_{m-2}) + b_{mn}^{(3)}}{(s-2m)(t-2n)}, \quad (\text{B.29})$$

where $b_{mn}^{(3)}$ are some coefficients that should in principle be fixed by $\log^2 U \log^2 V$ terms in the correlator. Even if we do not have access to them, we can still say that, in order to mix with the contributions coming from the $c_{mn}^{(3)}$, the $b_{mn}^{(3)}$ should show something in common and present a very constrained polynomial structure. For these reasons, we thought that it was worthwhile to study the flat space limit of (B.29) with $b_{mn}^{(3)} = 0$. After having regularized the sum, this reads

$$\partial_s^3 \partial_t^3 \iint dm dn \frac{7! 6^3 m^{11} (2p_3 (m/m+n) H_{-1-1} - q_3 (-m/n) H_{-1})}{n^3 (m+n)^3 (s-2m)(t-2n)}. \quad (\text{B.30})$$

Consistently to what we discussed before, we compared the integrand, without the s, t poles, to

$$\frac{1}{\pi^2} \text{[Diagram: A square with dashed lines forming a smaller square inside, and a vertical line through the center.]} = \frac{32s^{11} (p_3 (s/s+t) H_{-1-1} - q_3 (-s/t) H_{-1} - P_1(s, t))}{5t^3 (s+t)^3}. \quad (\text{B.31})$$

Again, notice the mismatch in the multiplicative coefficients of the highest transcendentality pieces. The reason behind it should again be found in the fact that we do not know triple trace operators contributions and we should in principle consider the $b_{mn}^{(3)}$. Similarly, if we integrate Eq. (B.30), we obtain part of the amplitude (or part of c_1 if we take its discontinuity) with the right weights, but with some mismatches. Nevertheless, all these similarities tell us that, at least in the flat space limit, the form of the full correlator is very constrained and that the unknown terms should mix with the studied ones in a very precise way and with a similar polynomial structure.

C Polynomial Structure

In Sec. 2.4 we have reported the expressions for the polynomials of the highest and next to the highest transcendental functions, namely p_κ and q_κ in Eqs. (2.50) and (2.51). The same contributions can be extracted from the iterated s -channel cut computations in Sec. 3.2, exploiting the iterative method we have developed. Let us now explain how we can extract the highest weight polynomials:

- the integrand is splitted into two regions, each one has an associated kernel $\mathcal{K}^\pm(v, x)$ where we have defined the adimensional parameter $x = t/s$. After each integration x is mapped to $1 - v$.
- we are interested in finding the poles, as those integrated will give the highest transcendental function;
- at each loop order only one of the two $\mathcal{K}^\pm(v, x)$ functions will contribute with a pole: the $-$ with a pole in $v = 0$ for the even loops and the $+$ with a pole in $v = 1$ for the odd ones;
- This pattern suggests that the highest transcendental function is a sequence of 0 and -1 .

The results obtained in this way reproduce the previous ones, in particular (remember that the loop order is equivalent to $\kappa - 1$)

$$\begin{cases} \frac{4^\kappa \kappa!}{15 \cdot 32} i^\kappa \frac{1}{x^3(1-x)^3} p_\kappa(-1/x) & \text{for } \kappa \text{ even} \\ \frac{4^\kappa \kappa!}{15 \cdot 32} i^{\kappa+1} \frac{1}{x^3(1-x)^3} p_\kappa(1/(1+x)) & \text{for } \kappa \text{ odd} \end{cases} \quad (\text{C.1})$$

We can play a similar game for the next transcendental piece, in this case the iterative structure is a bit more involved:

- both $\mathcal{K}^\pm(v, x)$ functions will contribute at each loop order;
- contrary to what happens before, now we have two contributions, one coming from the highest transcendental polynomial and one coming from the next to the highest at the previous loop;
- for the highest transcendental polynomial at even loop we have to obtain the general patter for the integration of

$$\frac{H_{0,\dots}(v-1)}{v^i} \quad H_{0,\dots}(v-1)v^i, \quad (\text{C.2})$$

for both $\mathcal{K}^\pm(v, x)$ functions in the associated integration regions $\{0, 1+x\}$ and $\{1+x, 1\}$.

- for odd loops we have to do the same but for a different set of functions and pole structure, namely:

$$\frac{H_{-1,\dots}(v-1)}{(v-1)^i} \quad H_{-1,\dots}(v-1)v^i. \quad (\text{C.3})$$

- The next to the highest transcendental piece at the previous order will contribute only when integrated against a simple pole in $\{v, (v-1)\}$. The pattern is similar to the one obtained for the highest transcendental polynomials just in this case the poles contributions are inverted²⁴.

²⁴This happens because contrary to the highest transcendental part where only x and $(1+x)$ can appear in the denominator at each loop for the next to the highest one both contributions appear.

As before we can express the results in terms of the q_κ 's:

$$\begin{cases} \frac{-4^\kappa \kappa!}{15 \cdot 32} i^\kappa \frac{1}{x^3(1-x)^3} q_\kappa(1/1+x) & \text{for } \kappa \text{ even} \\ \frac{4^\kappa \kappa!}{15 \cdot 32} i^{\kappa+1} \frac{1}{x^3(1-x)^3} q_\kappa(-1/x) & \text{for } \kappa \text{ odd} \end{cases} \quad (\text{C.4})$$

We notice that, as already in Eq. (2.49), the arguments of the p 's and q 's are alternating. In addition, if we translate these results in terms of $z = \frac{1}{1+x}$ we notice that the polynomials that we find from the amplitude correspond to the one multiplying I_κ and $I_{\kappa-1}$. Interestingly these integrals are the ones producing $\log^2 V$, confirming the connection between CFT logarithmic singularities and amplitudes, as we have explored in Mellin space in Sec. 4.1.

References

- [1] O. Aharony, L. F. Alday, A. Bissi, and E. Perlmutter, *Loops in AdS from Conformal Field Theory*, *JHEP* **07** (2017) 036, [[arXiv:1612.03891](#)].
- [2] S. M. Chester, M. B. Green, S. S. Pufu, Y. Wang, and C. Wen, *New Modular Invariants in $\mathcal{N} = 4$ Super-Yang-Mills Theory*, [arXiv:2008.02713](#).
- [3] S. M. Chester and S. S. Pufu, *Far Beyond the Planar Limit in Strongly-Coupled $\mathcal{N} = 4$ SYM*, [arXiv:2003.08412](#).
- [4] S. M. Chester, *Genus-2 holographic correlator on $AdS_5 \times S^5$ from localization*, *JHEP* **04** (2020) 193, [[arXiv:1908.05247](#)].
- [5] S. M. Chester, M. B. Green, S. S. Pufu, Y. Wang, and C. Wen, *Modular Invariance in Superstring Theory From $\mathcal{N} = 4$ Super-Yang-Mills*, [arXiv:1912.13365](#).
- [6] F. Aprile, J. Drummond, P. Heslop, and H. Paul, *One-loop amplitudes in $AdS_5 \times S^5$ supergravity from $\mathcal{N} = 4$ SYM at strong coupling*, *JHEP* **03** (2020) 190, [[arXiv:1912.01047](#)].
- [7] F. Aprile, J. Drummond, P. Heslop, H. Paul, F. Sanfilippo, M. Santagata, and A. Stewart, *Single Particle Operators and their Correlators in Free $\mathcal{N} = 4$ SYM*, [arXiv:2007.09395](#).
- [8] J. Drummond, R. Glew, and H. Paul, *One-loop string corrections for AdS Kaluza-Klein amplitudes*, [arXiv:2008.01109](#).
- [9] S. Komatsu, M. F. Paulos, B. C. Van Rees, and X. Zhao, *Landau diagrams in AdS and S-matrices from conformal correlators*, [arXiv:2007.13745](#).
- [10] A. Bissi, G. Fardelli, and A. Georgoudis, *Towards All Loop Supergravity Amplitudes on $AdS_5 \times S^5$* , [arXiv:2002.04604](#).
- [11] L. F. Alday and S. Caron-Huot, *Gravitational S-matrix from CFT dispersion relations*, *JHEP* **12** (2018) 017, [[arXiv:1711.02031](#)].

- [12] F. Aprile, J. Drummond, P. Heslop, and H. Paul, *Double-trace spectrum of $N = 4$ supersymmetric Yang-Mills theory at strong coupling*, *Phys. Rev. D* **98** (2018), no. 12 126008, [[arXiv:1802.06889](#)].
- [13] L. F. Alday, A. Bissi, and E. Perlmutter, *Genus-One String Amplitudes from Conformal Field Theory*, *JHEP* **06** (2019) 010, [[arXiv:1809.10670](#)].
- [14] L. F. Alday and X. Zhou, *Simplicity of AdS Supergravity at One Loop*, [arXiv:1912.02663](#).
- [15] L. F. Alday, *On Genus-one String Amplitudes on $AdS_5 \times S^5$* , [arXiv:1812.11783](#).
- [16] D. J. Binder, S. M. Chester, S. S. Pufu, and Y. Wang, *$\mathcal{N} = 4$ Super-Yang-Mills correlators at strong coupling from string theory and localization*, *JHEP* **12** (2019) 119, [[arXiv:1902.06263](#)].
- [17] J. Drummond and H. Paul, *One-loop string corrections to AdS amplitudes from CFT*, [arXiv:1912.07632](#).
- [18] T. Bargheer, F. Coronado, and P. Vieira, *Octagons II: Strong Coupling*, [arXiv:1909.04077](#).
- [19] J. Drummond, H. Paul, and M. Santagata, *Bootstrapping string theory on $AdS_5 \times S^5$* , [arXiv:2004.07282](#).
- [20] L. F. Alday and A. Bissi, *Loop Corrections to Supergravity on $AdS_5 \times S^5$* , *Phys. Rev. Lett.* **119** (2017), no. 17 171601, [[arXiv:1706.02388](#)].
- [21] F. Aprile, J. Drummond, P. Heslop, and H. Paul, *Quantum Gravity from Conformal Field Theory*, *JHEP* **01** (2018) 035, [[arXiv:1706.02822](#)].
- [22] F. Aprile, J. Drummond, P. Heslop, and H. Paul, *Unmixing Supergravity*, *JHEP* **02** (2018) 133, [[arXiv:1706.08456](#)].
- [23] D. Meltzer, E. Perlmutter, and A. Sivaramakrishnan, *Unitarity Methods in AdS/CFT*, *JHEP* **03** (2020) 061, [[arXiv:1912.09521](#)].
- [24] D. Meltzer and A. Sivaramakrishnan, *CFT Unitarity and the AdS Cutkosky Rules*, [arXiv:2008.11730](#).
- [25] R. J. Eden, P. V. Landshoff, D. I. Olive, and J. C. Polkinghorne, *The analytic S-matrix*. Cambridge Univ. Press, Cambridge, 1966.
- [26] G. P. Korchemsky, *On Near forward high-energy scattering in QCD*, *Phys. Lett. B* **325** (1994) 459–466, [[hep-ph/9311294](#)].
- [27] E. D’Hoker, M. B. Green, O. Gürdogan, and P. Vanhove, *Modular Graph Functions*, *Commun. Num. Theor. Phys.* **11** (2017) 165–218, [[arXiv:1512.06779](#)].
- [28] E. D’Hoker and M. B. Green, *Identities between Modular Graph Forms*, *J. Number Theor.* **189** (2018) 25–88, [[arXiv:1603.00839](#)].

- [29] E. D’Hoker, M. B. Green, and B. Pioline, *Higher genus modular graph functions, string invariants, and their exact asymptotics*, *Commun. Math. Phys.* **366** (2019), no. 3 927–979, [[arXiv:1712.06135](#)].
- [30] E. D’Hoker, M. B. Green, and B. Pioline, *Asymptotics of the $D^8\mathcal{R}^4$ genus-two string invariant*, *Commun. Num. Theor. Phys.* **13** (2019) 351–462, [[arXiv:1806.02691](#)].
- [31] E. D’Hoker and O. Schlotterer, *Identities among higher genus modular graph tensors*, [arXiv:2010.00924](#).
- [32] J. E. Gerken, A. Kleinschmidt, and O. Schlotterer, *Generating series of all modular graph forms from iterated Eisenstein integrals*, *JHEP* **07** (2020), no. 07 190, [[arXiv:2004.05156](#)].
- [33] J. E. Gerken, A. Kleinschmidt, C. R. Mafra, O. Schlotterer, and B. Verbeek, *Towards closed strings as single-valued open strings at genus one*, [arXiv:2010.10558](#).
- [34] M. Nirschl and H. Osborn, *Superconformal Ward identities and their solution*, *Nucl. Phys. B* **711** (2005) 409–479, [[hep-th/0407060](#)].
- [35] F. A. Dolan, L. Gallot, and E. Sokatchev, *On four-point functions of 1/2-BPS operators in general dimensions*, *JHEP* **09** (2004) 056, [[hep-th/0405180](#)].
- [36] C. Beem, L. Rastelli, and B. C. van Rees, *More $\mathcal{N} = 4$ superconformal bootstrap*, *Phys. Rev. D* **96** (2017), no. 4 046014, [[arXiv:1612.02363](#)].
- [37] G. Arutyunov and S. Frolov, *Four point functions of lowest weight CPOs in $N=4$ SYM(4) in supergravity approximation*, *Phys. Rev. D* **62** (2000) 064016, [[hep-th/0002170](#)].
- [38] F. Dolan and H. Osborn, *Superconformal symmetry, correlation functions and the operator product expansion*, *Nucl. Phys. B* **629** (2002) 3–73, [[hep-th/0112251](#)].
- [39] S. Caron-Huot and A.-K. Trinh, *All tree-level correlators in $AdS_5 \times S_5$ supergravity: hidden ten-dimensional conformal symmetry*, *JHEP* **01** (2019) 196, [[arXiv:1809.09173](#)].
- [40] I. Heemskerk, J. Penedones, J. Polchinski, and J. Sully, *Holography from Conformal Field Theory*, *JHEP* **10** (2009) 079, [[arXiv:0907.0151](#)].
- [41] T. Okuda and J. Penedones, *String scattering in flat space and a scaling limit of Yang-Mills correlators*, *Phys. Rev. D* **83** (2011) 086001, [[arXiv:1002.2641](#)].
- [42] J. Maldacena, D. Simmons-Duffin, and A. Zhiboedov, *Looking for a bulk point*, *JHEP* **01** (2017) 013, [[arXiv:1509.03612](#)].
- [43] M. Gary, S. B. Giddings, and J. Penedones, *Local bulk S-matrix elements and CFT singularities*, *Phys. Rev. D* **80** (2009) 085005, [[arXiv:0903.4437](#)].
- [44] S. Caron-Huot, *Analyticity in Spin in Conformal Theories*, *JHEP* **09** (2017) 078, [[arXiv:1703.00278](#)].

- [45] J. Liu, E. Perlmutter, V. Rosenhaus, and D. Simmons-Duffin, *d-dimensional SYK, AdS Loops, and 6j Symbols*, *JHEP* **03** (2019) 052, [[arXiv:1808.00612](#)].
- [46] R. E. Cutkosky, *Singularities and discontinuities of Feynman amplitudes*, *J. Math. Phys.* **1** (1960) 429–433.
- [47] Z. Bern, J. Carrasco, H. Johansson, and R. Roiban, *The Five-Loop Four-Point Amplitude of $N=4$ super-Yang-Mills Theory*, *Phys. Rev. Lett.* **109** (2012) 241602, [[arXiv:1207.6666](#)].
- [48] W. van Neerven, *Dimensional Regularization of Mass and Infrared Singularities in Two Loop On-shell Vertex Functions*, *Nucl. Phys. B* **268** (1986) 453–488.
- [49] G. Mack, *D-independent representation of Conformal Field Theories in D dimensions via transformation to auxiliary Dual Resonance Models. Scalar amplitudes*, [arXiv:0907.2407](#).
- [50] L. Rastelli and X. Zhou, *Mellin amplitudes for $AdS_5 \times S^5$* , *Phys. Rev. Lett.* **118** (2017), no. 9 091602, [[arXiv:1608.06624](#)].
- [51] L. Rastelli and X. Zhou, *How to Succeed at Holographic Correlators Without Really Trying*, *JHEP* **04** (2018) 014, [[arXiv:1710.05923](#)].
- [52] J. Penedones, *Writing CFT correlation functions as AdS scattering amplitudes*, *JHEP* **03** (2011) 025, [[arXiv:1011.1485](#)].
- [53] A. Fitzpatrick, J. Kaplan, J. Penedones, S. Raju, and B. C. van Rees, *A Natural Language for AdS/CFT Correlators*, *JHEP* **11** (2011) 095, [[arXiv:1107.1499](#)].
- [54] M. F. Paulos, *Towards Feynman rules for Mellin amplitudes*, *JHEP* **10** (2011) 074, [[arXiv:1107.1504](#)].
- [55] S. M. Chester and E. Perlmutter, *M-Theory Reconstruction from $(2,0)$ CFT and the Chiral Algebra Conjecture*, *JHEP* **08** (2018) 116, [[arXiv:1805.00892](#)].
- [56] M. Correia, A. Sever, and A. Zhiboedov, *An Analytical Toolkit for the S-matrix Bootstrap*, [arXiv:2006.08221](#).
- [57] H. Frellesvig and C. G. Papadopoulos, *Cuts of Feynman Integrals in Baikov representation*, *JHEP* **04** (2017) 083, [[arXiv:1701.07356](#)].
- [58] E. Remiddi and J. A. M. Vermaseren, *Harmonic polylogarithms*, *Int. J. Mod. Phys. A* **15** (2000) 725–754, [[hep-ph/9905237](#)].
- [59] D. Maitre, *HPL, a mathematica implementation of the harmonic polylogarithms*, *Comput. Phys. Commun.* **174** (2006) 222–240, [[hep-ph/0507152](#)].
- [60] D. Maitre, *Extension of HPL to complex arguments*, *Comput. Phys. Commun.* **183** (2012) 846, [[hep-ph/0703052](#)].

- [61] Z. Bern, L. J. Dixon, D. Dunbar, M. Perelstein, and J. Rozowsky, *On the relationship between Yang-Mills theory and gravity and its implication for ultraviolet divergences*, *Nucl. Phys. B* **530** (1998) 401–456, [[hep-th/9802162](#)].
- [62] M. B. Green, J. G. Russo, and P. Vanhove, *Modular properties of two-loop maximal supergravity and connections with string theory*, *JHEP* **07** (2008) 126, [[arXiv:0807.0389](#)].
- [63] A. V. Kotikov, *Differential equations method: New technique for massive Feynman diagrams calculation*, *Phys. Lett.* **B254** (1991) 158–164.
- [64] A. V. Kotikov, *Differential equation method: The Calculation of N point Feynman diagrams*, *Phys. Lett.* **B267** (1991) 123–127.
- [65] Z. Bern, L. J. Dixon, and D. A. Kosower, *Dimensionally regulated pentagon integrals*, *Nucl. Phys.* **B412** (1994) 751–816, [[hep-ph/9306240](#)].
- [66] E. Remiddi, *Differential equations for Feynman graph amplitudes*, *Nuovo Cim.* **A110** (1997) 1435–1452, [[hep-th/9711188](#)].
- [67] T. Gehrmann and E. Remiddi, *Differential equations for two loop four point functions*, *Nucl. Phys.* **B580** (2000) 485–518, [[hep-ph/9912329](#)].
- [68] J. M. Henn, *Multiloop integrals in dimensional regularization made simple*, *Phys. Rev. Lett.* **110** (2013) 251601, [[arXiv:1304.1806](#)].
- [69] C. G. Papadopoulos, *Simplified differential equations approach for Master Integrals*, *JHEP* **07** (2014) 088, [[arXiv:1401.6057](#)].
- [70] R. N. Lee, *Reducing differential equations for multiloop master integrals*, *JHEP* **04** (2015) 108, [[arXiv:1411.0911](#)].
- [71] J. Ablinger, A. Behring, J. Blümlein, A. De Freitas, A. von Manteuffel, and C. Schneider, *Calculating Three Loop Ladder and V-Topologies for Massive Operator Matrix Elements by Computer Algebra*, *Comput. Phys. Commun.* **202** (2016) 33–112, [[arXiv:1509.08324](#)].
- [72] C. G. Papadopoulos, D. Tommasini, and C. Wever, *The Pentabox Master Integrals with the Simplified Differential Equations approach*, *JHEP* **04** (2016) 078, [[arXiv:1511.09404](#)].
- [73] X. Liu, Y.-Q. Ma, and C.-Y. Wang, *A Systematic and Efficient Method to Compute Multi-loop Master Integrals*, *Phys. Lett.* **B779** (2018) 353–357, [[arXiv:1711.09572](#)].
- [74] K. Chetyrkin and F. Tkachov, *Integration by parts: The algorithm to calculate β -functions in 4 loops*, *Nuclear Physics B* **192** (1981), no. 1 159 – 204.
- [75] C. Meyer, *Algorithmic transformation of multi-loop master integrals to a canonical basis with CANONICA*, *Comput. Phys. Commun.* **222** (2018) 295–312, [[arXiv:1705.06252](#)].

- [76] J. Henn, B. Mistlberger, V. A. Smirnov, and P. Wasser, *Constructing d -log integrands and computing master integrals for three-loop four-particle scattering*, *JHEP* **04** (2020) 167, [[arXiv:2002.09492](#)].
- [77] M. Prausa, *epsilon: A tool to find a canonical basis of master integrals*, *Comput. Phys. Commun.* **219** (2017) 361–376, [[arXiv:1701.00725](#)].
- [78] O. Gituliar and V. Magerya, *Fuchsia: a tool for reducing differential equations for Feynman master integrals to epsilon form*, *Comput. Phys. Commun.* **219** (2017) 329–338, [[arXiv:1701.04269](#)].
- [79] M. Argeri, S. Di Vita, P. Mastrolia, E. Mirabella, J. Schlenk, U. Schubert, and L. Tancredi, *Magnus and Dyson Series for Master Integrals*, *JHEP* **03** (2014) 082, [[arXiv:1401.2979](#)].
- [80] O. V. Tarasov, *Connection between Feynman integrals having different values of the space-time dimension*, *Phys. Rev.* **D54** (1996) 6479–6490, [[hep-th/9606018](#)].
- [81] R. N. Lee, *Space-time dimensionality D as complex variable: Calculating loop integrals using dimensional recurrence relation and analytical properties with respect to D* , *Nucl. Phys.* **B830** (2010) 474–492, [[arXiv:0911.0252](#)].
- [82] R. N. Lee, *Calculating multiloop integrals using dimensional recurrence relation and D -analyticity*, *Nucl. Phys. Proc. Suppl.* **205-206** (2010) 135–140, [[arXiv:1007.2256](#)].
- [83] F. Dolan and H. Osborn, *Conformal partial wave expansions for $N=4$ chiral four point functions*, *Annals Phys.* **321** (2006) 581–626, [[hep-th/0412335](#)].
- [84] J. Bosma, K. J. Larsen, and Y. Zhang, *Differential equations for loop integrals in Baikov representation*, *Phys. Rev. D* **97** (2018), no. 10 105014, [[arXiv:1712.03760](#)].
- [85] F. Aprile and P. Vieira, *Large p explorations. From SUGRA to big STRINGS in Mellin space*, [arXiv:2007.09176](#).
- [86] J. Penedones, J. A. Silva, and A. Zhiboedov, *Nonperturbative Mellin Amplitudes: Existence, Properties, Applications*, *JHEP* **08** (2020) 031, [[arXiv:1912.11100](#)].